1 **Microbial dynamics in a High-Arctic glacier forefield: a combined field, laboratory, and modelling**

2 **approach.**

3 James A. Bradley [1,2], Sandra Arndt [2], Marie Šabacká [1], Liane G. Benning [3,4], Gary L. Barker [5], Joshua

4 J. Blacker [3], Marian L. Yallop [5], Katherine E. Wright [1], Christopher M. Bellas [1], Jonathan Telling [1], Martyn

5 Tranter [1], Alexandre M. Anesio [1]

6

7 [1] Bristol Glaciology Centre, School of Geographical Sciences, University of Bristol, BS8 1SS, UK

8 [2] BRIDGE, School of Geographical Sciences, University of Bristol, BS8 1SS, UK

9 [3] School of Earth and Environment, University of Leeds, LS2 9JT, UK

10 [4] GFZ, German Research Centre for Geosciences, 14473 Potsdam, Germany

11 [5] School of Biological Sciences, University of Bristol, BS8 1SS, UK

12

13 Corresponding author: James A. Bradley, email: j.bradley@bristol.ac.uk

14

15 **Abstract:** Modelling the development of soils in glacier forefields is necessary in order to assess how

16 microbial and geochemical processes interact and shape soil development in response to glacier

17 retreat. Furthermore, such models can help us predict microbial growth and the fate of Arctic soils in an

18 increasingly ice-free future. Here, for the first time, we combined field sampling with laboratory analyses

19 and numerical modelling to investigate microbial community dynamics in oligotrophic proglacial soils in

20 Svalbard. We measured low bacterial growth rates and growth efficiencies (relative to estimates from

21 Alpine glacier forefields), and high sensitivity to soil temperature (relative to temperate soils). We used

22 these laboratory measurements to inform parameter values in a new numerical model and significantly

23 refined predictions of microbial and biogeochemical dynamics of soil development over a period of

24 roughly 120 years. The model predicted the observed accumulation of autotrophic and heterotrophic

25 biomass. Genomic data indicated that initial microbial communities were dominated by bacteria derived

26 from the glacial environment, whereas older soils hosted a mixed community of autotrophic and

27 heterotrophic bacteria. This finding was simulated by the numerical model, which showed that active

28 microbial communities play key roles in fixing and recycling carbon and nutrients. We also demonstrated

29 the role of allochthonous carbon and microbial necromass in sustaining a pool of organic material,

30 despite high heterotrophic activity in older soils. This combined field, laboratory and modelling approach

31 demonstrates the value of integrated model-data studies to understand and quantify the functioning of

32 the microbial community in an emerging High-Arctic soil ecosystem.

33

34 **Key words**

35 Glacier forefield

36 Microbial dynamics

37 Soil development

38 Numerical modelling

39 Integrated field-laboratory-modelling

40 SHIMMER

1. Introduction

Polar regions are particularly sensitive to anthropogenic climate change (Lee, 2014) and have experienced accelerated warming in recent decades (Johannessen et al., 2004; Serreze et al., 2000; Moritz et al., 2002). The response of terrestrial Polar ecosystems to this warming is complex, and research to understand the response of terrestrial ecosystems in high latitudes to environmental change is of increasing importance. A visible consequence of Arctic warming is the large-scale retreat of glacier and ice cover (ACIA, 2005; Paul et al., 2011; Staines et al., 2014; Dyurgerov and Meier, 2000). From underneath the ice, a new terrestrial biosphere emerges, playing host to an ecosystem which may exert an important influence on biogeochemical cycles, and more specifically atmospheric CO_2 concentrations and associated climate feedbacks (Dessert et al., 2003; Anderson et al., 2000; Smittenberg et al., 2012; Berner et al., 1983).

Numerous studies have attempted to characterize the physical and biological development of recently exposed soils using a chronosequence approach, whereby a transect perpendicular to the retreating ice snout represents a time sequence with older soils at increasing distance from the ice snout (Schulz et al., 2013). We have recently shown that microbial biomass and macronutrients (such as carbon, phosphorus and nitrogen) can accumulate in soils over timescales of decades to centuries (Bradley et al., 2014). In such pristine glacial forefield soils the activity of microbial communities is thought to be responsible for this initial accumulation of carbon and nutrients. Such an accumulation facilitates colonization by higher order plants, leading to the accumulation of substantial amounts of organic carbon (Insam and Haselwandter, 1989). However, organic carbon may also be derived from allochthonous sources such as material deposited on the soil surface (from wind, hydrology, precipitation and ornithogenic sources) and ancient organic pools derived from under the glacier (Schulz et al., 2013). Nevertheless, the relative significance of allochthonous and autochthonous sources of carbon to forefield soils, as well as their effect on ecosystem behaviour are so far still poorly understood (Bradley et al., 2014). Moreover, cycling of bioavailable nitrogen (which is derived from active nitrogen-fixing organisms, allochthonous deposition, and degradation of organic substrates) and phosphorus (liberated from the weathering of minerals and decomposition of organic substrates) are similarly poorly quantified.

Several studies have observed shifts in the microbial community inhabiting pro-glacial soils of various ages (Zumsteg et al., 2012; Zumsteg et al., 2011). This was expressed in increasing rates of autotrophic and bacterial production with soil age (Schmidt et al., 2008; Zumsteg et al., 2013; Esperschutz et al., 2011; Frey et al., 2013) and the overall decline in quality of organic substrates in older soils (Goransson et al., 2011; Insam and Haselwandter, 1989). However, current evidence is limited to mostly descriptive approaches, which may be challenging to interpret due to inherent difficulties in disentangling interacting microbial and geochemical processes across various temporal and spatial scales. Furthermore, the inherent heterogeneity of glacial forefield soils makes the development of a single conceptual model that fits all challenging. Accordingly, pro-glacial biogeochemical processes that dominate such systems

81 remain poorly quantified and highly under-explored. This current lack of understanding limits our ability
82 to predict the future evolution of these emerging landscapes and the potential consequences on global
83 climate. Numerical models present an opportunity to expand our knowledge of glacier forefield
84 ecosystems by analytically testing the hypotheses that arise from observations, extrapolating,
85 interpolating and budgeting processes, rates and other features to explore beyond the possibility of
86 empirical observation (Bradley et al., 2016). With such a model we can then also explore the sensitivity
87 and resilience of these ecosystems to environmental change.
88
89 Here, we have combined field observations, with laboratory incubations and elemental measurements
90 as well as genomic analyses and used these in a numerical model to investigate the development of
91 soils in a glacial forefield. The present study forms an important part of the integrated and iterative
92 model-data approach outlined in the model description and testing (Bradley et al, 2015) whereby initial
93 model development was informed by decades of empirical research, new data and laboratory
94 experiments (presented here) are used to refine and inform model simulations, and so forth. With this
95 data we refined some model parameters in the recently developed *S*oil biogeoc*H*em*I*cal *M*odel for
96 *M*icrobial *E*cosystem *R*esponse (SHIMMER 1.0; Bradley et al. (2015)) model and applied this to the
97 emerging forefield of the Midtre Lovénbreen glacier in Svalbard. Pioneer soils in the High-Arctic and
98 Antarctica, such as the Midtre Lovénbreen forefield, are ideal sites to test this field-laboratory-model
99 approach due to the lack of vegetation during initial stages of soil development, as the presence of
100 vegetation would obscure the microbial community dynamics and considerably alter the physical
101 properties of the soil (Brown and Jumpponen, 2014; Ensign et al., 2006; King et al., 2008; Kastovska
102 et al., 2005; Schutte et al., 2009; Duc et al., 2009). The model development was informed by decades
103 of empirical research on glacier forefield soils, and has already been tested and validated using
104 published datasets from the Damma Glacier in Switzerland and the Athabasca Glacier in Canada. A
105 thorough sensitivity analysis highlighted the most important parameters to constrain in order to make
106 further predictions more robust. All our model parameter values are specific to individual, local model
107 conditions and inherently contain necessary model simplifications, abstractions and assumptions.
108 Nevertheless, our earlier sensitivity analyses revealed the following highly sensitive key parameters as
109 the most important to constrain through measurements: the maximum heterotrophic growth rate (I_{maxH}),
110 the bacterial growth efficiency (BGE, parameter Y_H) and the temperature response (Q_{10}).
111
112 Therefore, in this current study, we combined detailed field measurements with specifically designed
113 laboratory experiments and quantified values for these three parameters with a specific set of soils from
114 for the Midtre Lovénbreen forefield. The laboratory experiments and measurements were conducted
115 with the objective to better constrain these sensitive parameters. We then ran model simulations in
116 order to explore the ranges of model output and refine model predictions compared to the previous
117 range identified in Bradley et al (2015). Next, we examined model output to explore the microbial and
118 biogeochemical dynamics of recently exposed soils in the Midtre Lovénbreen catchment and evaluate
119 two main hypotheses. First, we tested the hypothesis that microbial biomass in recently exposed soils
120 accumulates due to *in situ* bacterial growth and activity. It is commonly observed in glacier forefields

that microbial biomass accumulates with increasing soil age following exposure (Bernasconi et al., 2011; Schulz et al., 2013; Bradley et al., 2014). This study provides a new quantitative and process-focused approach to examine *in situ* growth in pioneer ecosystems, and assess the role of different functional groups in biomass accumulation. Second, we tested the hypothesis that carbon fluxes in very recently exposed soils are low, and are dominated by (abiotic) deposition of allochthonous substrate, whereas carbon fluxes are high in older soils due to increased microbial (biotic) activity (such as microbial growth, respiration and cell death). Increased soil carbon fluxes with soil age have been linked to microbial activity from the forefield of the Damma Glacier, Switzerland (Smittenberg et al., 2012; Guelland et al., 2013b). With this combined model, field and lab study, we were able to estimate carbon fluxes between ecosystem components with daily resolution, and provide new insight into the interplay of processes that contribute to net ecosystem production and soil organic carbon stocks in a High-Arctic system.

2. Methods

2.1. Study site and sampling

Midtre Lovénbreen is an Arctic polythermal valley glacier on the south side of Kongsfjorden, Western Svalbard (latitude 78°55'N, longitude 12°10'E) (Fig. 1). The Midtre Lovénbreen catchment is roughly 5 km East of Ny-Ålesund, where several long-term monitoring programs have provided a wealth of contextual information. Midtre Lovénbreen has experienced negative mass balance throughout much of the 20th century. Since the end of the Little Ice Age (maximum in Svalbard in the 1900s) the de-glaciated surface area of the Midtre Lovénbreen catchment has increased considerably in response to warming mean annual temperatures. This continues to the present day. Between 1966 and 1990 ~ 2.3 km^2 of land was exposed (Fleming et al., 1997; Moreau et al., 2008). We used a chronosequence approach to determine ages for soils based on satellite imagery (Landsat TM 7) and previously determined soil ages by aerial photography and carbon-14 dating techniques in Hodkinson et al. (2003). Soil samples were collected along a transect perpendicular to the glacier snout, representing soil ages of 0, 3, 5, 29, 50, and 113 years (Fig. 1) during the field season (18 July to 29 August 2013). At each of the 6 sites along the chronosequence, 10 meter traverses roughly parallel to the glacier snout were established and at each site 3 soil plots were sampled (using ethanol sterilized sampling equipment). After removing the > 2 cm rock pieces at each site, about 100 grams of soil was collected from the top 15 cm and immediately placed into sterile high-density polyethylene bags (Whirl-Pak (Lactun, Australia)) and into a cool box partially filled with cool packs and dry ice. Samples were immediately frozen and stored at -20°C on return to the UK Arctic Research station in Ny-Ålesund (no longer than 5 hours after collection). Samples were transported frozen on dry ice to the laboratories in the Universities of Bristol and Leeds (UK).

2.2. Laboratory analyses

For bacterial abundance, samples were thawed and aliquots (100 mg) were immediately transferred into sterile 1.5 mL micro-centrifuge (Eppendorf) tubes, where they were diluted with 900 µL of Milli-Q water (0.2 µm filtered) and immediately fixed in 100 µL glutaraldehyde (0.2 µm filtered, 2.5% final

161 concentration). Samples were then vortexed for 10 seconds and sonicated for 1 minute at 30°C to
162 facilitate cell detachment from soil particles. Then 10 µL fluorochrome DAPI (4', 6-diamidino-2
163 phenylindole) was added to half of the samples, tubes were vortexed briefly (3 seconds) and incubated
164 in the dark for 10 minutes, to be counted under UV light. The other half of each sample remained
165 untreated, for counting under auto-fluorescent light for photosynthetic pigmentation. Samples were
166 vortexed for 10 seconds and let stand for a further 30 seconds to ensure a well-mixed solution, prior to
167 filtering 100 µL of the mixed liquid sample onto black Millipore Isopore membrane filters (0.2 µm pore
168 size, 25 mm diameter), rinsed with a further 250 µL of Milli-Q water (0.2 µm filtered). Bacterial cells were
169 then counted using an Olympus BX41 microscope at 1000 times magnification. The filtering apparatus
170 was washed out with Milli-Q water between each filtration, and negative control samples, prepared
171 using Milli-Q water, were included into each series. A negative control was a sample with no visible
172 stained or auto-fluorescing cells. Thirty random grids (each 10^4 µm^2) were counted per sample. Cell
173 morphologies were measured and cell volume was estimated and converted to carbon content
174 according to Bratbak and Dundas (1984) (see Supplementary Information). Separate aliquots of soil
175 from each site were weighed after thawing and then dried at 105°C to obtain an estimate of soil moisture
176 content.
177
178 Environmental DNA was isolated from at least 3 replicates for each soil age using MoBio PowerMax ®
179 Soil DNA Isolation Kit and by following the instruction manual. 5 to 10 g of soil was used per sample to
180 isolate DNA. Following extraction, DNA was diluted to equimolar concentrations, so that all samples
181 contained 7.0 ng of DNA, prior to amplification. The isolated genomic DNA was amplified with bacterial
182 primers 515f (5'-GTGYCAGCMGCCGCGGTAA-3') and 926r (5'-CCGYCAATTYMTTTRAGTTT-3')
183 (Caporaso et al., 2012), creating a single amplicon of ~400 bp. The reaction was carried out in 50 µL
184 volumes containing 0.3 mg mL^{-1} Bovine Serum Albumin, 250 µM dNTPs, 0.5 µM of each primer, 0.02
185 U Phusion High-Fidelity DNA Polymerase (Finnzymes OY, Espoo, Finland) and 5x Phusion HF Buffer
186 containing 1.5 mM MgCl$_2$. The following PCR conditions were used: initial denaturation at 95°C for 5
187 minutes, followed by 25 cycles consisting of denaturation (95°C for 40 seconds), annealing (55°C for 2
188 minutes) and extension (72°C for 1 minute) and a final extension step at 72°C for 7 minutes. Following
189 amplification, all amplicons were normalized to the same concentration (9.0 ng) before sequencing.
190 Samples were sequenced using the Ion Torrent platform (using Ion 318v2 chip) at Bristol Genomics
191 facility at the University of Bristol. Samples were barcoded in the PCR stage and demultiplexed in QIIME
192 using split_libraries.py code (Caporaso et al., 2010). A non-barcoded library was prepared from the
193 amplicon pool using Life technologies Short Amplicon Prep Ion Plus Fragment Library Kit. The template
194 and sequencing kits used were: Ion PGM Template OT2 400 Kit and Ion PGM Sequencing 400 kit. The
195 sequencing yielded 4.38 million reads. The 16S sequences were further processed using MOTHUR (v.
196 1.35) and QIIME pipelines (Schloss et al., 2009; Caporaso et al., 2010). Initially, low quality or too long
197 and too short sequences were removed in MOTHUR. Chimeric sequences were identified and removed
198 using UCHIME (Edgar et al., 2011). QIIME was used to cluster reads into operational taxonomical units
199 (OTUs) using the pick_closed_reference_otus.py command. The final OTU table contained between
200 2329-43269 reads for each sample. The varying sequence coverage among samples was adjusted by

201 normalizing the OTU matrix to the same total abundance of sequences for each sample (2329) using
202 the command normalize_table.py in QIIME. Sequences were clustered into OTUs based on at least
203 97% sequence similarity, and assigned taxonomical identification against Greengenes bacterial
204 database (McDonald et al., 2012). The result was a biom format file containing the taxonomic
205 information for each OTU as well as OTU frequency per sample. Sequence data is available on NCBI
206 under project ID PRJNA341831, and individual accession numbers are provided in the Supplementary
207 Information.

208

209 The carbon contents in the year 0 soils were analysed with a Carlo-Erba elemental analyser (NC2500)
210 at the German Research Center for Geosciences, Potsdam, Germany. The soils were oven dried at
211 40°C for 48 hours, sieved to <7 mm and crushed using a TEMA disk mill to achieve size fractions of <
212 20 µm. Total organic carbon (TOC) was analysed after reacting the powders with a 10% HCl solution
213 for 12 hours to remove inorganic carbonates.

214

215 **2.3. Determination of maximum growth rates**
216 The microbial activity was determined in 113 year old soil samples after they were thawed (in the dark
217 at 5°C to mimic typical field temperature) for 168 hours. This age was chosen because these soil
218 samples were assumed to be the ones with the highest microbial biomass and activity and thus the
219 most practical for all laboratory measurements. In order to mitigate the effect of variability derived from
220 differences in soil properties between soil ages (that will later be predicted by the model), laboratory
221 experiments were conducted on a single soil age, with replicate incubations to assess the possible
222 variability in rates (and thus parameter values) that can be attributed to experimental procedures and
223 measurement techniques.

224

225 Aliquots of the soils were divided into petri dishes (25 g of soil (wet weight) into each petri dish) for
226 subsequent treatments. In order to alleviate nutrient limitations and measure maximum growth rates,
227 four different nutrient conditions were simulated: (1) no addition of nutrients, (2) low (0.03 mg C g^{-1},
228 0.008 mg N g^{-1}, 0.02 mg P g^{-1}), (3) medium (0.8 mg C g^{-1}, 0.015 mg N g^{-1}, 0.1 mg P g^{-1}) and (4) high
229 additions (2.4 mg C g^{-1}, 0.024 mg N g^{-1}, 0.3 mg P g^{-1}). The ranges and concentrations were informed
230 by similar experiments in recently exposed proglacial soils at the Damma Glacier, Switzerland
231 (Goransson et al., 2011). Nutrients ($C_6H_{12}O_6$ for C, NH_4NO_3 for N and KH_2PO_4 for P) (Sigma, quality
232 ≥99.0%) were dissolved in 2 mL Milli-Q water (0.2 µm filtered), and mixed into the soils using an ethanol-
233 sterilized spatula. Samples were incubated in the dark for a further 72 hours with the lids on at 25°C,
234 the reference temperature (T_{ref}) at which all rates are defined in SHIMMER prior to adjustment with the
235 temperature dependency expression (using Q_{10}) (Bradley et al., 2015). In order to derive a value for
236 I_{maxH}, we were obligated to perform growth incubations at T_{ref} (25°C) despite this being a more typical
237 soil temperature of Alpine soils rather than High-Arctic soils (see Fig. S3 (c)). However, we are confident
238 that by deriving a Q_{10} value based on incubations of the same soils encapsulating typical (5°C) to high
239 (25°C) soil temperatures, we can numerically derive appropriate actual growth rates from the maximum
240 growth rate (at T_{ref}). We are confident that the major outcomes and conclusions of this study are not

241 affected by high incubation temperatures since measured growth rates at high temperatures are
242 appropriately scaled using the Q_{10} formulation as measured experimentally. Throughout the whole
243 incubation time, at 24 hour intervals, additional 2 mL aliquots of Milli-Q water (0.2 μm filtered) were
244 added to maintain approximate soil moisture conditions in each sample.

246 In these samples bacterial production was estimated by the incorporation of ^{3}H-leucine using the
247 microcentrifuge method detailed in Kirchman (2001). After the initial 72 hour incubation period
248 quadruplicate sample aliquots from the petri dish incubations and two trichloroacetic acid (TCA) killed
249 control samples were incubated for 3 hours at T_{ref} (25°C) for every nutrient treatment. Approximately
250 50 mg of soil was transferred to sterile micro-centrifuge tubes (2.0 mL, Fischer Scientific). Milli-Q (0.2
251 μm pre-filtered) water and ^{3}H-leucine was added to a final concentration of 100 nM (optimum leucine
252 concentration was pre-determined by a saturation experiment, Fig. S1, Supplementary Information).
253 The incubation was terminated by the addition of TCA to each tube. Tubes were then centrifuged at
254 15,000 g for 15 minutes, the supernatant was aspirated with a sterile pipette and removed, and 1 ml
255 ice-cold 5% TCA was added to each tube. Tubes were then centrifuged again at 15,000g for 5 minutes,
256 before again aspirating and removing the supernatant. 1mL ice-cold 80% ethanol was added and tubes
257 were centrifuged at 15,000 g for 5 minutes, before the supernatant was aspirated and removed again
258 and tubes were left to air dry for 12 hours. Finally, 1 mL of scintillation cocktail was added, samples
259 were vortexed, and then counted by liquid scintillation (Perkin Elmer Liquid Scintillation Analyzer, Tri-
260 Carb 2810 TR). Radioisotope activity of TCA-killed control samples was always less than 1.1% of the
261 measured activity in live samples. There was a positive correlation between the amount of sediment
262 added to the tubes and background counts representing disintegrations per minute (DPM). Counts were
263 individually normalized by the amount of sediments (corrected for dry weight) used in each sample to
264 discount for background DPM. Leucine incorporation rates were converted into bacterial carbon
265 production following the methodology of Simon and Azam (1989). Bacterial abundance was estimated
266 from each treatment after the 72 hour incubation period by microscopy. Five samples from each petri
267 dish were counted for each nutrient treatment with negative controls yielding no detectable cells. One-
268 way ANOVA (with post-hoc Tukey HSD) statistical tests were used for evaluations of the variability from
269 the multiple treatments.

271 **2.4. Temperature response**
272 Microbial community respiration was determined by measuring CO_2 gas exchange rates in airtight
273 incubation vials. Soil samples from the 113 year old site were defrosted and divided (25 g wet weight)
274 in petri dishes as above, and 2 mL of Milli-Q water (0.2 μm filtered) was added (to maintain consistency
275 of soil moisture with determination of bacterial production above). Samples were incubated at 5°C (T_1)
276 and 25°C (T_2) in the dark for a further 72 hours. 2mL of 0.2 μm pre-filtered Milli-Q water was added to
277 the T_1 sample (3 mL for T_2) at 24, 48 and 72 hours to maintain approximate soil moisture content. Two
278 separate killed control tests (one furnaced at 450°C for 4 hours, and one autoclaved (3 cycles at 121°C))
279 were incubated at T_1 and T_2. Quintuple live and killed samples (roughly 1 g) were transferred into
280 cleaned 20 mL glass vials (rinsed in 2% Decon, submersed in 10% HCl for 24 hours, rinsed 3 times

281 with Milli-Q water and furnaced at 450°C for 4 hours). These were sealed (9°C, atmospheric pressure,
282 ambient CO_2 of 405 ppm) with pre-sterilized Bellco butyl stoppers (pre-sterilized by boiling for 4 hours
283 in 1M sodium hydroxide) and crimped shut with aluminium caps. Sealed vials were then incubated at
284 T_1 and T_2 for 24 hours in darkness. After 24 hours, the headspace gas was removed with a gas-tight
285 syringe and immediately analysed on an EGM4 gas analyser (PP Systems, calibrated using gas
286 standards matching the expected range, precision 1.9%, 2*SE). Empty pre-sterilized vials were also
287 incubated and analysed. Following gas analysis, vials were opened and dried to a constant weight at
288 105°C to estimate moisture content and thus dry soil weight of these aliquots. Headspace CO_2 change
289 (ppm) was converted to microbial respiration using the ideal gas law (n=PV/RT), assuming negligible
290 changes in soil pore water pH (and therefore CO_2 solubility) during the incubation. CO_2 headspace
291 changes resulting from killed controls and blanks were < 70% of the changes resulting from the
292 incubations at T_1, and <7% of the changes observed at T_2. One-way ANOVA (with post-hoc Tukey
293 HSD) statistical tests were used for comparison of multiple treatments. No significant differences in CO_2
294 headspace change between killed controls at T_1 and T_2 were detected (P=0.95).
295
296 **2.5. Microbial Model: SHIMMER**
297 SHIMMER (Bradley et al., 2015) mechanistically describes and predicts transformations in carbon,
298 nitrogen and phosphorus through aggregated components of the microbial community as a system of
299 interlinked ordinary differential equations. The model contains pools of microbial biomass, organic
300 matter and both dissolved inorganic and organic nitrogen and phosphorus (Table 1). It categorizes
301 microbes into autotrophs (A_{1-3}) and heterotrophs (H_{1-3}), and further subdivides these based on 3 specific
302 functional traits. Microbes derived from underneath the glacier (referred to as "glacial microbes") are
303 termed A_1 and H_1. A_1 are chemolithoautotrophic, obtaining energy from the oxidation and reduction of
304 inorganic compounds and carbon from the fixation of carbon dioxide. In contrast, H_1 rely on the
305 breakdown of organic molecules for energy to support growth. A_2 and H_2 represent autotrophic and
306 heterotrophic microbes commonly found in glacier forefield soils with no "special" characteristics, and
307 will be referred to as "soil microbes". A_3 and H_3 are autotrophs and heterotrophs that are able to fix
308 atmospheric N_2 gas as a source of nitrogen in cases when dissolved inorganic nitrogen (DIN) stocks
309 become limiting. Available organic substrate is assumed to be derived naturally from dead organic
310 matter and allochthonous inputs. Labile compounds are immediately available fresh and highly reactive
311 material, rapidly turned over by the microorganisms (S_1, ON_1, OP_1). Refractory compounds are less
312 bioavailable and represents the bulk of substrate present in the non-living organic component of soil
313 (S_2, ON_2, OP_2). A conceptual diagram showing the components and transfers of SHIMMER is presented
314 in the Supplementary Information (Fig. S2).
315
316 Microbial biomass responds dynamically to changing substrate and nutrient availability (expressed as
317 Monod-kinetics), as well as changing environmental conditions (such as temperature and light). A Q_{10}
318 temperature response function (T_f) is affixed to all metabolic processes including growth rates and death
319 rates (Bradley et al., 2015), thus effectively slowing down or speeding up all life processes as
320 temperature changes (Soetaert and Herman, 2009; Yoshitake et al., 2010; Schipper et al., 2014). Light

limitation is expressed as Monod kinetics. The following external forcings drive and regulate the system's dynamics:

- Photosynthetically-active radiation (PAR) (wavelength of approximately 400 to 700 nm) (W m^{-2}).
- Snow depth (m).
- Soil temperature (°C).
- Allochthonous inputs (µg g^{-1} day^{-1}).

The model is 0-D and represents the soil as a homogeneous mix. Thus, light, temperature, nutrients, organic compounds and microbial biomass are assumed to be evenly distributed.

Soil temperature (at 1 cm depth) for the entire of 2013 is provided by Alfred Wegener Institute for Polar and Marine Research (AWI) from the permafrost observatory near Ny-Ålesund, Svalbard. Similarly, PAR for 2013 are measured at the AWI surface radiation station near Ny-Ålesund, Svalbard. Averaged daily snow depth for 2009 to 2013 is provided by the Norwegian Meteorological Institute (eKlima). Allochthonous nutrient fluxes (inputs and leaching) are estimated based on an evaluation of nutrient budgets of the Midtre Lovénbreen catchment (Hodson et al., 2005) in which budgets for nutrient deposition rates and runoff concentrations are measured over two full summer-winter seasons and residual retention rates (excess of inputs) or depletion rates (excess of outputs) are inferred. The bioavailability of allochthonous material is assumed to be the same as initial material and microbial necromass.

Initial conditions were informed by analysis of 0-years-of-exposure soil collected adjacent to the ice snout, and initial values for all state variables are presented in Table 1. Initial microbial biomass was estimated by microscopy as described above. Initial community structure was derived by 16S analysis of year-0 soils. An initial value for carbon substrate ($S_1 + S_2$) was estimated based on the average TOC content of year-0 soil. Bioavailability of model TOC was assumed to be 30% labile (S_1) and 70% refractory (S_2) (for consistency with Bradley et al. (2015)). Organic nitrogen (ON) and organic phosphorus (OP) were assumed to be stoichiometrically linked by the measured C:N:P ratio from the Damma Glacier forefield (from which the model was initially developed and tested (Bradley et al., 2015)). An initial value for DIN was taken from a previous evaluation of Svalbard tundra nitrogen dynamics, whereby the lowest value is taken to represent the soil of least development, according to traditional understanding of glacier forefields (Alves et al., 2013; Bradley et al., 2014). An initial value for dissolved inorganic phosphorous (DIP) was established stoichiometrically from previous model development and testing.

Model implementation and set-up is described in more detail in the Supplementary Information.

2.6. Model parameters

360 Maximum heterotrophic growth rate I_{maxH} (day^{-1}) was estimated by scaling the measured rate of bacterial

361 production (µg C g^{-1} day^{-1}) (converted to dry weight) with total heterotrophic biomass (µg C g^{-1}). Nutrient

362 addition alleviates growth limitations as defined in SHIMMER (Bradley et al., 2015); thus bacterial

363 communities can be assumed to be growing at I_{maxH} under experimental conditions.

364

365 Y_H represents heterotrophic BGE, and was estimated according to the equation:

366

367 $$Y_H = \frac{BP}{BP + BR}$$

368 (1)

369 Where BP is and BR are measured bacterial production and measured bacterial respiration (µg C g^{-1}

370 day^{-1}) respectively, at 25°C with no nutrients added.

371

372 The temperature response (Q_{10}) value was estimated as:

373

374 $$Q_{10} = \left(\frac{R_2}{R_1}\right)^{\left(\frac{10}{T_2 - T_1}\right)}$$

375 (2)

376 Where R_1 and R_2 represent the measured respiration rate (µg C g^{-1} day^{-1}) at temperatures T_1 and T_2

377 (5°C and 25°C).

378

379 Laboratory-defined parameters (i.e. growth rate, temperature sensitivity and BGE) were assumed to be

380 the same for all microbial groups. A complete list of parameters and values is presented in Table S3

381 (Supplementary Information).

382

383 **3. Results**

384 **3.1. Laboratory results and model parameters**

385 Bacterial production in untreated soil was estimated at 0.76 µg C g^{-1} day^{-1} (SD=0.12), and across all

386 nutrient treatments ranged from 0.560 to 2.196 µg C g^{-1} day^{-1}. Nutrient addition led to increased

387 measured production (low = 0.69 µg C g^{-1} day^{-1} (SD=0.12), medium = 1.09 µg C g^{-1} day^{-1} (SD=0.53),

388 high = 1.52 µg C g^{-1} day^{-1} (SD=0.63)), however variability between replicates was also high and

389 production rates from each nutrient treatment were not significantly different from untreated soil

390 (P_{low}=0.99, P_{medium}=0.70, P_{high}=0.10). The increased bacterial production was cross-correlated with

391 quadruplicate measurements of biomass from each treatment, and resulting growth rate coefficients

392 (I_{maxH}) for all treatments were within a narrow range (0.359 to 0.550 day^{-1}) and there was no statistically

393 significant difference in growth rates between each nutrient treatment (Fig. 2b) ($P_{low-medium}$=0.55, $P_{medium-}$

394 $_{high}$=0.49, $P_{none-high}$=0.10). The maximum measured growth rate for a single nutrient treatment, thus

395 equating to the parameter I_{maxH}, was 0.55 day^{-1}. The 95% confidence range for I_{maxH} is 0.50 to 0.60 day^{-}

396 ^{1}. This value is, to our knowledge, is the first measured rate of bacterial growth from High-Arctic soils,

397 and falls within the lower end of the plausible range established in Bradley et al. (2015) (0.24 – 4.80

398 day^{-1}) (Fig. 3a) for soil microbes from a range of laboratory and modelling studies (Frey et al., 2010;

Ingwersen et al., 2008; Knapp et al., 1983; Zelenev et al., 2000; Stapleton et al., 2005; Darrah, 1991; Blagodatsky et al., 1998; Vandewerf and Verstraete, 1987; Foereid and Yearsley, 2004; Toal et al., 2000; Scott et al., 1995). For respiration, significantly higher CO_2 headspace concentration were detected in the live incubations at 25°C relative to killed controls (P < 0.05). Average respiration rate at 5°C was 1.61 µg C g^{-1} day^{-1} and there was a significant increase in soil respiration at 25°C (12.83 µg C g^{-1} day^{-1}) (Fig. 2c) (P < 0.05). The Q_{10} value for Midtre Lovénbreen forefield soils was thus calculated as 2.90, and a 95% confidence range was established as 2.65 to 3.16. This was at the upper end of the plausible range previously identified in Bradley et al. (2015) (Fig. 3b). Based on measured values of bacterial production and respiration, BGE (Y_H) was 0.06, with a 95% confidence range of 0.05 to 0.07 (Fig. 3c). Final calculated values for model parameters are summarized in Table S3 (Supplementary Information).

The results from microscopy determination of biomass are presented in Table 2. In the freshly exposed soil (year 0) heterotrophic biomass was low (0.059 µg C g^{-1}), increased substantially to 0.244 µg C g^{-1} in 29 year old soils, and was an order or magnitude higher (2.00 µg C g^{-1}) in 113 year old soils. Autotrophic biomass was considerably higher than heterotrophic biomass and increased by roughly an order of magnitude from year 0 (0.171 µg C g^{-1}) to year 29 (1.07 µg C g^{-1}) and approximately doubled by year 113 (2.58 µg C g^{-1}). TOC in freshly exposed soil was approximately 0.793 mg C g^{-1}).

16S data was categorized into microbial groups (A_{1-3} and H_{1-3}) as defined by the model formulation. Chemolithoautotrophs, such as known iron or sulphur oxidizers (genera *Acidothiobacillus*, *Thiobacillus*, *Gallionella*, *Sulfurimonas*) were assigned into the A_1 group. Phototrophic microorganisms, such as cyanobacteria (*Phormidium*, *Leptolyngbya*) and phototrophic bacteria (*Rhodoferax*, *Erythrobacter*, *Halomicronema*) were allocated into group A_2, while heterocyst forming cyanobacteria from the orders Nostocales and Stigonematales were assigned to group the A_3 (nitrogen-fixing autotrophs). Members of the family Comamonadaceae of the Betaproteobacteria are known glacial dwelling microorganisms (Yde et al., 2010) and were thus included into the group H_1. General soil heterotrophic microorganisms (mainly members of Alphaproteobacteria, Actinobacteria, Bacterioidetes and Acidobacteria) were assigned into group H_2 (general soil heterotrophs). Lastly, group H_3 consisted of heterotrophic nitrogen fixers, mainly *Azospirillum*, *Bradyrhizobium*, *Devosia*, *Clostridium*, *Frankia* and *Rhizobium*. Pathogens, non-soil microorganisms and organisms with unknown physiological traits were assigned into the "Uncategorized" group. Glacial microbes accounted for 43 to 45 % of reads in year 0 and 5, and declined in older soils (year 50 and 113) to 18 to 22%. The glacial community was predominantly chemolithoautotrophic (A_1). Typical soil bacteria (A_2 and H_2) increased from low abundance (30% and 40% in years 0 and 5 respectively) to relatively high abundance (63 to 67% of reads) in years 50 and 113. Nitrogen fixing bacteria were prevalent in recently exposed soils (14% in year 0) but low in relative abundance in soils above 5 years of age (4 to 6% in years 5, 50 and 113). In the freshly exposed soil (year 0), the microbial community was relatively evenly distributed between heterotrophs (43%) and autotrophs (44%). In developed soils, the relative abundance of heterotrophs increased (up to 74% of

reads in years 50 and 113). Important to note is the fact that between 8 and 21% of the reads across all samples could not be classified.

3.2. Model Results

The model predicted an accumulation of autotrophic and heterotrophic biomass over 120 years (Fig. 4a and 4b). Biomass and nutrient concentrations were initially extremely low (total biomass < 0.25 µg C g^{-1}, DIN < 4.0 µg N g^{-1}, DIP < 3.0 µg P g^{-1}), and biological activity in initial soils was also low (Table 3). There was an order of magnitude increase in total microbial biomass in years 10 to 60. Nitrogen-fixing autotrophs (A_3) and heterotrophs (H_3), and soil heterotrophs (H_2) experienced rapid growth during this period. Glacial and soil autotrophs (A_{1-2}) and glacial heterotrophs (H_1) remained low. Bacterial production increased by roughly two orders of magnitude (Table 3). Organic carbon (labile and refractory) increased (Fig. 4c), whilst DIN and DIP concentrations increased by approximately an order of magnitude in the first 60 years (Fig. 4d). During the later stages of soil development (years 60 to 120), biomass increased rapidly due to the rapid growth of soil organisms (A_2 and H_2), which outcompeted nitrogen-fixers. The model showed a rapid exhaustion of labile organic carbon (years 50 to 100), while refractory carbon accumulated slowly. Nutrients (DIN and DIP) accumulated at a relatively constant rate. Microbial activity, including bacterial production, nitrogen fixation and DIN assimilation, was high relative to early stages (Table 3).

A carbon budget of fluxes through the substrate pool is presented in Fig. 5. Daily fluxes are presented in panels (a) for year 5, (b) for year 50 and (c) for year 113, and annual fluxes up to year 120 are presented in (d). In recently exposed soils (5 years), allochthonous inputs were the only noticeable carbon flux, outweighing heterotrophic growth and respiration, and the contribution of substrate from necromass and exudates by over two orders of magnitude (Fig. 5a). Thus, the total change in carbon (black line) closely resembled allochthonous input. In the intermediate stages (Fig. 5b), there was substantial depletion from the substrate pool due to heterotrophic activity. Heterotrophic growth (red line) was low despite high substrate consumption and respiration (dark blue line). In the late stages of soil development, the flux of microbial necromass was a significant contributor to the organic substrate pools (Fig. 5c). Carbon fluxes in mid to late stages of soil development were highly seasonal (Fig. 5b and 5c). Biotic fluxes (e.g. respiration) were up to six times higher during the summer (July to September) compared to the winter (November to April), however a base rate of heterotrophic respiration and turnover of microbial biomass was sustained over winter. Figure 4d shows that the contribution of microbial necromass rose steadily throughout the simulation (light blue line), however was not sufficient to compensate the uptake of carbon substrate, thus leading to overall depletion between years 50 to 110 (black line). The contribution of exudates (purple line) to substrate was minimal at all soil ages.

4. Discussion

4.1. Determination of parameters and model predictions

477   Figure 6 illustrates the influence of the site-specific, laboratory-derived parameters on microbial
478   biomass predictions. It compares the range of predicted microbial biomass based on laboratory-
479   determined parameters (yellow) to the entire plausible parameter range (red; Bradley et al. (2015)).
480   Predicted biomass with the average laboratory-derived value is indicated by the black line. For I_{max},
481   predicted biomass with laboratory-derived parameters (yellow shading) was towards the lower end of
482   the plausible range (Fig. 6a) because refined growth rates were significantly lower than the maximum
483   values explored previously. This was mostly due to a significant reduction in autotrophic biomass (A_{1-}
484    $_3$). With high growth rates, there was a sharp early increase in biomass (years 10 to 20) followed by
485   slower growth phase (years 20 to 120). Model results with laboratory-derived growth rates showed that
486   the exponential growth phase occurred later (years 40 to 80) and was more prolonged, but total biomass
487   was considerably lower. There was a substantial reduction in the plausible range in predicted microbial
488   biomass.
489
490   There was a substantial reduction in the plausible range in predicted microbial biomass (Fig. 6b) from
491   the measured temperature sensitivity (Q_{10}) (yellow) compared to the previous range (red). Soil microbial
492   communities in Polar regions must contend with extremely harsh environmental conditions such as cold
493   temperatures, frequent freeze-thaw cycles, low water availability, low nutrient availability, high exposure
494   to ultraviolet radiation in the summer, and prolonged periods of darkness in winter. These factors
495   profoundly impact their metabolism and survival strategies and ultimately shape the structure of the
496   microbial community (Cary et al., 2010). High Q_{10} values, as derived here, are typical of cold
497   environments and cold adapted organisms and this has been associated with the survival of biomass
498   under prolonged periods of harsh environmental conditions (Schipper et al., 2014). An investigation into
499   the metabolism of microbial communities in biological soils crusts in recently exposed soils from the
500   Austre Broggerbreen Glacier, approximately 6 km from the Midtre Lovénbreen catchment, also derived
501   a high Q_{10} (3.1) (Yoshitake et al., 2010). The Midtre Lovénbreen catchment, in Svalbard, experiences
502   a relatively extreme Arctic climate. The high Q_{10} ultimately lowers the overall rate of biomass
503   accumulation in ultra-oligotrophic soils and a baseline population is maintained.
504
505   The low measured BGE (0.06) suggested that a high proportion (94%) of substrate consumed by
506   heterotrophs is remineralized (degrading organic substrate into DIC (CO_2), DIN and DIP), with very little
507   being incorporated into biomass (6%). Low BGE encouraged the liberation and release of nutrients to
508   the soil and thus the overall growth response of the total microbial biomass was more rapid due to
509   higher soil nutrient concentrations (Fig. 6c). However, due to the low BGE, there was a high rate of
510   substrate degradation, and as such, labile substrate was rapidly depleted when heterotrophic biomass
511   was high (Fig. 4c). Heterotrophic growth requires that a substantial amount of substrate is degraded –
512   thus, although autotrophic production outweighed heterotrophic production at all stages of development
513   (Fig. 4e), the soil was predicted by the model to be a net source of CO_2 to the atmosphere over the first
514   120 years of exposure (Fig. 4f). Heterotrophic growth and respiration (and thus net ecosystem
515   production and carbon fluxes) are strongly dependant on the availability of soil organic carbon. Poorly
516   quantified rates of allochthonous organic carbon deposition and its quality may lead to generally high

517 uncertainty in the net ecosystem production due to potentially enhanced heterotrophic growth resulting
518 from higher organic carbon deposition, or lower heterotrophic growth resulting from substrate limitation
519 in low-deposition scenarios. Soil CO_2 efflux is highly sensitive to variable net ecosystem production,
520 thus simulated net ecosystem production estimates must be interpreted cautiously until sufficient field
521 data emerges (e.g. from in situ measurement of soil gas exchange). The calculation of BGE assumes
522 that bacterial respiration is the major contributor to measured CO_2 gas exchange rates from soil
523 microcosms. In reality, all active and living soil organisms are likely to contribute to measured CO_2
524 fluxes, however due to limitations with experimental protocols, it is extremely difficult to determine the
525 relative contribution of various organisms to total respiration. Microscopy analysis showed limited
526 presence of fungi and protozoa suggesting that the biological community of the soil community is mainly
527 bacterial. Nevertheless, by attributing total measured CO_2 fluxes solely to bacteria, BGE may be under-
528 estimated (due to an overestimation of respiration rates attributed to the bacterial community). Thus,
529 we cannot exclude that our low BGE values might be in part an artefact of this experimental limitation.
530 However, although there are very few measurements of BGE in cold glaciated environments, our
531 estimate of BGE is in good agreement with previous studies, which have suggested values ranging
532 between 0.0035 and 0.033 (Anesio et al., 2010; Hodson et al., 2007). Therefore, we are confident that
533 BGE values measured here fall within a realistic range.
534
535 Three assumptions are made in the assignment of measured parameters to SHIMMER as applied to
536 the High-Arctic field site. The first assumption of SHIMMER is that parameter values remain constant
537 throughout the duration of the simulation. Empirical evidence suggests that parameters defined as fixed
538 in SHIMMER (e.g. Q_{10}) may be variable over time, however in SHIMMER, like many numerical
539 modelling formulations, changing environmental (temperature, light) and geochemical (carbon
540 substrate, available nitrogen, available phosphorus) conditions drive subsequent variability in microbial
541 activity via mathematical formulations (e.g. Monod kinetics, see Bradley et al. (2015)) affixed to
542 parameter values. A second assumption is the assignment of measured rates to parameters for all
543 microbial functional groups. Rather than taxonomic based classification, SHIMMER distinguishes and
544 classifies microbial communities based on functional traits. These mathematical formulations assigned
545 to, for example, microbial growth, are different between groups to represent distinct functional traits
546 associated with that group. Whilst actual rates may be different between different organisms, for the
547 level of model complexity and outputs required, a community measurement of those parameters is
548 sufficient, particularly considering that the differences are accounted for in the mathematical formulation
549 of SHIMMER (see Bradley et al. (2015)). Third, maximum microbial growth rate at T_{ref} (25°C, Bradley
550 et al. (2015)) as modelled in SHIMMER is modified by Monod terms that account for nutrient limitation
551 (e.g. Monod terms), as well as a temperature response function (Q_{10}) to estimate actual growth rate at
552 ambient temperature. A major objective of of this study was to improve model performance by
553 constraining previously identified key model parameters (see sensitivity study results in Bradley at al.
554 (2015)) through specifically designed laboratory experiments. We showed this by comparing model
555 simulation results applying measured, site-specific parameter with simulation results using a range of
556 parameter values reported in the literature (Fig. 6).

4.2. Microbial biomass dynamics and community structure

Measured microbial biomass in the initial soils of Midtre Lovénbreen (0.23 µg C g^{-1}, 0 years) was very low compared to initial soils in other deglaciated forefields of equivalent ages in lower latitudes, for example in the Alps (4 µg C g^{-1}) (Bernasconi et al., 2011; Tscherko et al., 2003) and Canada (6 µg C g^{-1}) (Insam and Haselwandter, 1989). However, our microbial biomass values are more similar to other recently deglaciated soils in Antarctica (Ecology Glacier - 0.88 µg C g^{-1}) (Zdanowski et al., 2013). Low biomass is possibly a result of the harsh, ultra-oligotrophic and nutrient limiting environment of the High Arctic and Antarctica, where low temperature and longer winters limit the summer growth phase, especially compared to an Alpine system (Tscherko et al., 2003; Bernasconi et al., 2011).

The initial microbial community structure in our samples was predominantly autotrophic (74.5%). In the years following exposure, we observed an increase in autotrophs and heterotrophs with soil age (Table 2), presumably due to the establishment and growth of stable soil microbial communities (Schulz et al., 2013; Bradley et al., 2014). Both the observations and modelling results suggested that there was no substantial increase in heterotrophic biomass during the initial and early-intermediate stages of soil development (years 0 to 40), which was then followed by a growth phase whereby biomass increased by roughly an order of magnitude. Overall, the model and the microscopy data were in good agreement accounting for the limitations in both techniques, spatial heterogeneity, and the oscillations in biomass arising from seasonality (Fig. 7). SHIMMMER predicted that low initial microbial populations have the potential to considerably increase in population density during several decades of soil development. This data thus supports the hypothesis that the observed increase in microbial biomass with soil age is a consequence of *in situ* growth and activity. The pattern of microbial abundance observed in the Midtre Lovénbreen forefield broadly resembles that of other glacier forefields worldwide (see Bradley et al. (2014)). For example, data from the Rootmoos Ferner (Austria) (Insam and Haselwandter, 1989), Athabasca (Canada) (Insam and Haselwandter, 1989), Damma (Switzerland) (Bernasconi et al., 2011; Schulz et al., 2013) and Puca (Peru) (Schmidt et al., 2008) glacier forefields find increased microbial biomass and activity over decades to centuries of soil development following exposure.

The genomic data indicated that glacial microbes (such as members of the family Comamonadaceae.) are dominant in recently exposed soils, in agreement with model results (Fig. 8). The community structure in year 5 was heavily dominated by chemolithoautotrophs (A$_1$) (including taxa *Thiobacillus*, *Rhodoplanes*, *Acidithiobacillus*, *Nitrospira*, *Sulfurimonas* and others), which reflected findings from previous studies whereby chemolithoautotrophic bacteria contribute to the oxidation of FeS$_2$ in proglacial moraines in Midtre Lovénbreen (Borin et al., 2010; Mapelli et al., 2011). These processes are also commonly described in other subglacial habitats (Boyd et al., 2014; Hamilton et al., 2013). Based on 16S data, the glacial community declined in relative abundance with soil age. This finding was also reflected in the model in years 50 and 113. As the age of the soil progressed, there was typically greater abundance of microbes representing typical soil bacteria (groups A$_2$ and H$_2$ including taxa *Geobacter*, *Micrococcus*, *Actinoplanes*, *Sphingomonas*, *Pedobacter* and *Devosia*, *Frankia*, *Rhizobium*) in the 16S

597   data and the model, thus the relative abundance of glacial microbes decreased. Relative abundance of
598   microbial communities across the chronosequence is plotted at the phylum and genus level in the
599   Supplementary Information (Fig. S4 and S5). The overall trends show the relative increase in the
600   proportion of Acidobacteria with the soil age. They contain typical soil bacteria and are thus often used
601   as markers of soil formation and soil development. They are usually associated with plant covered older
602   soils with lower pH as they specialize in degradation of plant recalcitrant organic compounds. The
603   younger soils, on the other hand contained relatively higher proportion of sequences of Proteobacteria
604   (particularly Betaproteobacteria), Bacterioidetes and Cyanobacteria, i.e. groups often associated with
605   supra or subglacial habitats.

606

607   Microscopic analyses indicated low total biomass in recently exposed soils (up to 1.7 μg C g^{-1} in soil
608   exposed for 50 years) that was comprised predominantly of autotrophic bacteria. Model simulations
609   agreed well with microscopy derived data. Overall, the 16S data, when categorised into functional
610   groups as defined by the model, agreed well with the microscopy and model output in the very early
611   stages of soil development. However, in later stages of soil development (50 years and older),
612   microscopy and modelling suggested a continuation of predominantly autotrophic soil microbial
613   communities whereas 16S sequence data notably indicated a predominantly heterotrophic community.
614   With extremely low biomass, cell counts derived from microscopy, as well as representation of relative
615   abundance by 16S extraction and amplification, can be largely skewed by relatively small changes in
616   the soil microbial community. Furthermore, the comparative difficulty to lyse autotrophic bacteria (such
617   as some groups of cyanobacteria) from an environmental sample compared to heterotrophic bacteria,
618   and thus successfully amplify the 16S gene during the PCR process, may skew 16S sequence data in
619   favour of heterotrophic sequence reads. Incomplete sample depth (shown by rarefaction curves, Fig
620   S6), the differential extractability of DNA from different organisms, and variation in rDNA copy number
621   adds potential for error to the presented 16S data, and thus absolute numbers should be treated with
622   caution. SHIMMER is an ambitious model in that it attempts to simulate, predict and constrain multiple
623   functional types of bacteria species in a numerical framework. Numerical models containing multiple
624   species or multiple microbial functional groups are often extremely challenging to constrain (Servedio
625   et al., 2014; Hellweger and Bucci, 2009; Jessup et al., 2004; Larsen et al., 2012), and as such, the
626   majority of microbial soil models often only resolve one or two living biomass pool that represents the
627   bulk activity and function of the entire community (see e.g. Manzoni et al. (2004), Manzoni and
628   Porporato (2007), Blagodatsky and Richter (1998), Ingwersen et al. (2008), Wang et al. (2014) and
629   others). Our rationale for resolving six distinct functional groups was to quantitatively assess, using
630   modelling, the relative importance and role of each functional group at different stages of soil
631   development. Regardless of discrepancies in older soils (over 50 years since exposure), both the 16S
632   and microscopy data indicated that there was a mixed community of autotrophs and heterotrophs in
633   soils of all ages, which was supported by modelling, since no functional groups were extirpated over
634   simulations representing 120 years of soil development. Thus, SHIMMER is able to capture the diversity
635   of the samples over 120 years of soil development, but the detailed community composition requires
636   further investigation.

637

Nitrogen-fixing bacteria such as *Nostoc, Rivularia, Pseudanabaena* and *Rhodobacter* were prevalent in recently exposed soils but declined in relative abundance with soil age. By fixing N_2 instead of assimilating DIN, the model predicted that nitrogen-fixers were able to grow rapidly in the early stages relative to other organisms (Fig. 4a, 4b). The model prediction supports findings by previous studies demonstrating the importance of nitrogen fixation in Alpine (Duc et al., 2009; Schmidt et al., 2008) and Antarctic (Strauss et al., 2012) glacier forefields and other High-Arctic (Svalbard, Greenland) glacial ecosystems (Telling et al., 2011; Telling et al., 2012). However, there was poor agreement on the relative abundance of nitrogen-fixers between the model and the 16S data in the later stages of soil development (years 50 to 120), particularly between autotrophs and heterotrophs. The model over-predicted the relative abundance of nitrogen-fixing organisms (Fig. 8). The majority of the biomass of the autotrophic nitrogen-fixers was composed of sequences belonging to the cyanobacterium from the genus *Nostoc. Nostoc* forms macroscopically visible colonies that grow on the surface of the soils. Its distribution in the Arctic soils is thus extremely patchy and therefore, part of the discrepancy between the 16S data and the model regarding the relative distribution of the A_3 group in the older soils could be due to under-sampling of the *Nostoc* colonies as a consequence of a random sampling approach. Furthermore, allochthonous inputs of nitrogen to the Arctic (e.g. aerial deposition (Geng et al., 2014)) strongly affect the productivity of microbial ecosystems and the requirement of nitrogen fixation for microbes (Bjorkman et al., 2013; Kuhnel et al., 2013; Kuhnel et al., 2011; Hodson et al., 2010; Telling et al., 2012; Galloway et al., 2008). Thus, uncertainty in the allochthonous availability of nitrogen strongly affects nitrogen fixation rates. In attempting to replicate a qualitative understanding of the nitrogen cycle in a quantitative mathematical modelling framework, the predicted importance of nitrogen-fixing organisms may be over-estimated. The poor agreement in the relative abundance of nitrogen-fixers between the model and the 16S data indicates an incomplete understanding of allochthonous versus autochthonous nutrient availability. Allochthonous nutrient availability is a known source of uncertainty (Bradley et al., 2014; Schulz et al., 2013; Schmidt et al., 2008), and addressing this concern is the subject of future work.

16S data is an exciting resource of information that is rarely (or never) used to test numerical process-based biogeochemical models. However, the environment (difficulty to extract DNA), the presentation (percentages of low concentration and thus easy to shift relative abundance), the potentially high proportion of dead or dormant cells (which may be present in sequence data but are not necessarily metabolically active), the differential extractability of DNA from different organisms and variation in rDNA copy number, and uncertainties in model formulation make comparisons challenging. In making this first attempt at comparison of model output to 16S data, we hope to spark discussion and further development of approaches that have similar objectives in order to improve future model performance.

4.3. Net ecosystem metabolism and carbon budget

677   Allochthonous carbon inputs were the most significant contributor to recently exposed soils (e.g. year
678   5), since the total change in substrate closely followed this flux (Fig. 5). In older soils (year 113), biotic
679   fluxes were substantially higher, and microbial necromass contributed equally as a source of organic
680   substrate compared to allochthonous deposition. In the older soils, heterotrophic growth and respiration
681   caused substantial consumption and thus depletion of available carbon stocks. This evidence thus
682   supports the hypothesis that carbon fluxes in very recently exposed soils are low and are dominated by
683   abiotic processes (i.e. allochthonous deposition), whereas biotic processes (such as microbial growth,
684   respiration and cell death) play a greater role in developed soils with increased microbial abundance
685   and activity. These findings for the Midtre Lovénbreen glacier in the High-Arctic, are similar to what has
686   been observed based on empirical evidence from Alpine settings (at the Damma Glacier, Switzerland
687   (Smittenberg et al., 2012; Guelland et al., 2013)).

689   The seasonality of carbon fluxes predicted by the model (Fig. 5b and 5c) related to the high measured
690   Q_{10} values. High seasonal variation in biotic fluxes and rates is typical of cryospheric soil ecosystems
691   (Schostag et al., 2015) including Alpine glacier forefield soils (Lazzaro et al., 2012; Lazzaro et al., 2015).
692   However, microbial activity has been shown to persist during winter under insulating layers of snow and
693   in sub-zero temperatures (Zhang et al., 2014). Modelling also predicted sustained organic substrate
694   degradation, microbial turnover and net heterotrophy during the winter (Fig. 5b and 5c), as documented
695   in other glacier forefield studies from an Alpine setting (Guelland et al., 2013b).

697   The low measured BGE has three important consequences. Firstly, low BGE suggests that a large pool
698   of substrate is required to support heterotrophic growth. Low-efficiency heterotrophic growth lead to the
699   rapid depletion of substrate; therefore high allochthonous inputs were required to maintain a sizeable
700   pool. In older soils (years 80 to 120), increased inputs from microbial necromass (blue line, Fig. 5d)
701   sustained substrate supply to heterotrophs. The sources of allochthonous carbon substrate to the
702   glacier forefield include meltwater inputs derived from the supraglacial and subglacial ecosystems
703   (Stibal et al., 2008; Hodson et al., 2005; Mindl et al., 2007), snow algae (which are known to be prolific
704   primary colonizers and producers in High Arctic snow packs (Lutz et al., 2015; Lutz et al., 2014),
705   atmospheric deposition (Kuhnel et al., 2013) and ornithogenic deposition (e.g. faecal matter of birds
706   and animals) (Jakubas et al., 2008; Ziolek and Melke, 2014; Luoto et al., 2015; Michelutti et al., 2009;
707   Michelutti et al., 2011; Moe et al., 2009). Microbial dynamics are moderately sensitive to external
708   allochthonous inputs of substrate (Bradley et al., 2015), and addressing the uncertainty associated with
709   this flux is an important question to address in future research.

711   Secondly, low BGE causes a net efflux of CO_2 over the first 120 years of soil development despite high
712   autotrophic production (Fig. 4e and 4f). Recent literature has explored the carbon dynamics of glacier
713   forefield ecosystems, finding highly variable soil respiration rates (Bekku et al., 2004; Schulz et al.,
714   2013; Guelland et al., 2013a). Future studies should focus on quantifying carbon and nutrient
715   transformations and the potential for forefield systems to impact global biogeochemical cycles in
716   response to future climate change (Smittenberg et al., 2012) and in the context of large-scale ice retreat.

717

718 Thirdly, high rates of substrate degradation encouraged by low BGE were responsible for rapid nutrient

719 release. Modelling suggested that microbial growth was strongly inhibited by low nutrient availability in

720 initial soils (4 µg N g^{-1}, 2 to 10 µg P g^{-1}) (Fig. 4d). This is consistent with findings from the Hailuogou

721 Glacier (Gongga Shan, China) and Damma Glacier (Switzerland) (Prietzel et al., 2013). Low BGE is

722 predicted by the model to have a very important role in encouraging the release of nutrients from organic

723 material more rapidly, thereby increasing total bacterial production in the intermediate stages of soil

724 development. Increased nutrient availability with increased heterotrophic biomass is consistent with

725 recent observations from glacier forefields (Bekku et al., 2004; Schulz et al., 2013; Schmidt et al., 2008).

726

727 **5. Conclusions**

728 We used laboratory-based mesocosm experiments to measure three key model parameters: maximum

729 microbial growth rate (I_{max}) (by incorporation of ^{3}H-leucine), BGE (Y) (by measuring respiration rates)

730 and the temperature response (Q_{10}) (by measuring rates at different ambient temperatures).

731 Laboratory-derived parameters were comparable with previous estimations. We refined model

732 predictions constraining site-specific parameters by lab experiments, thus decreasing parameter

733 uncertainty and narrowing the range of model output over nominal environmental conditions. A

734 comparison of model simulations using laboratory-derived parameter values and previously defined

735 parameter values showed that the coupling of high Q_{10} values and low BGE were important factors in

736 controlling biomass accumulation due to promoting survival of biomass during periods of low

737 temperature, and the enhanced recycling of nutrients through organic matter degradation, respectively.

738 Our results demonstrated that *in situ* microbial growth lead to the overall accumulation of microbial

739 biomass in the Midtre Lovénbreen forefield during the first century of soil development following

740 exposure. Furthermore, carbon fluxes increased in older soils due to elevated biotic (microbial) activity.

741 Microbial dynamics at the initial stages of soil development in glacial forefields do not contribute to

742 significant accumulation of organic carbon due to the very low growth efficiency of the microbial

743 community, resulting in a net efflux of CO_2 from those habitats. However, the low bacterial growth

744 efficiency in glacial forefields is also responsible for high rates of nutrient remineralization that most

745 probably has an important role on the establishment of plants at older ages. The relative importance of

746 allochthonous versus autochthonous substrate and nutrients is the focus of future research.

747

748 This exercise shows how an integrated model-data approach can improve understanding and

749 predictions of microbial dynamics in forefield soils and disentangle complex process interactions to

750 ascertain the relative importance of each process independently. This would, for annual budgets, be

751 extremely challenging with a purely empirical approach. Nevertheless, more clarity and data are needed

752 in tracing the dynamics and interactions of these carbon pools to improve confidence and validate model

753 simulations. Proglacial zones are expanding due to accelerated ice retreat. Thus, glacier forefields are

754 becoming an increasingly important novel habitat for microorganisms in glaciated regions experiencing

755 rapid changes in climate. This combined approach explored detailed microbial and biogeochemical

756 dynamics of soil development with the view to obtaining a more holistic picture of soil development in a
757 warmer and increasingly ice-free future world.
758

759 **Acknowledgements**

767
768

769 **References**

770 ACIA: Arctic Climate Impacts Assessment, Cambridge University Press, Cambridge, 1042,
771 2005.
772 Alves, R. J. E., Wanek, W., Zappe, A., Richter, A., Svenning, M. M., Schleper, C., and Urich, T.:
773 Nitrification rates in Arctic soils are associated with functionally distinct populations of
774 ammonia-oxidizing archaea, Isme J, 7, 1620-1631, 10.1038/ismej.2013.35, 2013.
775 Anderson, S. P., Drever, J. I., Frost, C. D., and Holden, P.: Chemical weathering in the foreland
776 of a retreating glacier, Geochim Cosmochim Ac, 64, 1173-1189, Doi 10.1016/S0016-
777 7037(99)00358-0, 2000.
778 Anesio, A. M., Sattler, B., Foreman, C., Telling, J., Hodson, A., Tranter, M., and Psenner, R.:
779 Carbon fluxes through bacterial communities on glacier surfaces, Ann Glaciol, 51, 32-40, 2010.
780 Bekku, Y. S., Nakatsubo, T., Kume, A., and Koizumi, H.: Soil microbial biomass, respiration rate,
781 and temperature dependence on a successional glacier foreland in Ny-Alesund, Svalbard, Arct
782 Antarct Alp Res, 36, 395-399, 2004.
783 Bernasconi, S. M., Bauder, A., Bourdon, B., Brunner, I., Bunemann, E., Christl, I., Derungs, N.,
784 Edwards, P., Farinotti, D., Frey, B., Frossard, E., Furrer, G., Gierga, M., Goransson, H., Gulland,
785 K., Hagedorn, F., Hajdas, I., Hindshaw, R., Ivy-Ochs, S., Jansa, J., Jonas, T., Kiczka, M.,
786 Kretzschmar, R., Lemarchand, E., Luster, J., Magnusson, J., Mitchell, E. A. D., Venterink, H. O.,
787 Plotze, M., Reynolds, B., Smittenberg, R. H., Stahli, M., Tamburini, F., Tipper, E. T., Wacker, L.,
788 Welc, M., Wiederhold, J. G., Zeyer, J., Zimmermann, S., and Zumsteg, A.: Chemical and
789 Biological Gradients along the Damma Glacier Soil Chronosequence, Switzerland, Vadose
790 Zone J, 10, 867-883, Doi 10.2136/Vzj2010.0129, 2011.
791 Berner, R. A., Lasaga, A. C., and Garrels, R. M.: The Carbonate-Silicate Geochemical Cycle and
792 Its Effect on Atmospheric Carbon-Dioxide over the Past 100 Million Years, Am J Sci, 283, 641-
793 683, 1983.
794 Bjorkman, M. P., Kuhnel, R., Partridge, D. G., Roberts, T. J., Aas, W., Mazzola, M., Viola, A.,
795 Hodson, A., Strom, J., and Isaksson, E.: Nitrate dry deposition in Svalbard, Tellus B, 65, Artn
796 19071
797 Doi 10.3402/Tellusb.V65i0.19071, 2013.
798 Blagodatsky, S. A., and Richter, O.: Microbial growth in soil and nitrogen turnover: A
799 theoretical model considering the activity state of microorganisms, Soil Biol Biochem, 30,
800 1743-1755, Doi 10.1016/S0038-0717(98)00028-5, 1998.

Blagodatsky, S. A., Yevdokimov, I. V., Larionova, A. A., and Richter, J.: Microbial growth in soil and nitrogen turnover: Model calibration with laboratory data, Soil Biol Biochem, 30, 1757-1764, Doi 10.1016/S0038-0717(98)00029-7, 1998.

Borin, S., Ventura, S., Tambone, F., Mapelli, F., Schubotz, F., Brusetti, L., Scaglia, B., D'Acqui, L. P., Solheim, B., Turicchia, S., Marasco, R., Hinrichs, K. U., Baldi, F., Adani, F., and Daffonchio, D.: Rock weathering creates oases of life in a High Arctic desert, Environ Microbiol, 12, 293-303, DOI 10.1111/j.1462-2920.2009.02059.x, 2010.

Boyd, E. S., Hamilton, T. L., Havig, J. R., Skidmore, M. L., and Shock, E. L.: Chemolithotrophic Primary Production in a Subglacial Ecosystem, Appl Environ Microb, 80, 6146-6153, 10.1128/Aem.01956-14, 2014.

Bradley, J. A., Singarayer, J. S., and Anesio, A. M.: Microbial community dynamics in the forefield of glaciers, Proceedings. Biological sciences / The Royal Society, 281, 2793-2802, 10.1098/rspb.2014.0882, 2014.

Bradley, J. A., Anesio, A. M., Singarayer, J. S., Heath, M. R., and Arndt, S.: SHIMMER (1.0): a novel mathematical model for microbial and biogeochemical dynamics in glacier forefield ecosystems, Geosci. Model Dev., 8, 3441-3470, 10.5194/gmd-8-3441-2015, 2015.

Bradley, J. A., Anesio, A., and Arndt, S.: Bridging the divide: a model-data approach to Polar & Alpine Microbiology, Fems Microbiol Ecol, 92, 10.1093/femsec/fiw015, 2016.

Bratbak, G., and Dundas, I.: Bacterial Dry-Matter Content and Biomass Estimations, Appl Environ Microb, 48, 755-757, 1984.

Brown, S. P., and Jumpponen, A.: Contrasting primary successional trajectories of fungi and bacteria in retreating glacier soils, Mol Ecol, 23, 481-497, Doi 10.1111/Mec.12487, 2014.

Caporaso, J. G., Kuczynski, J., Stombaugh, J., Bittinger, K., Bushman, F. D., Costello, E. K., Fierer, N., Pena, A. G., Goodrich, J. K., Gordon, J. I., Huttley, G. A., Kelley, S. T., Knights, D., Koenig, J. E., Ley, R. E., Lozupone, C. A., McDonald, D., Muegge, B. D., Pirrung, M., Reeder, J., Sevinsky, J. R., Tumbaugh, P. J., Walters, W. A., Widmann, J., Yatsunenko, T., Zaneveld, J., and Knight, R.: QIIME allows analysis of high-throughput community sequencing data, Nat Methods, 7, 335-336, 10.1038/nmeth.f.303, 2010.

Caporaso, J. G., Lauber, C. L., Walters, W. A., Berg-Lyons, D., Huntley, J., Fierer, N., Owens, S. M., Betley, J., Fraser, L., Bauer, M., Gormley, N., Gilbert, J. A., Smith, G., Knight, R.: Ultra-high-throughput microbial community analysis on the Illumina HiSeq and MiSeq platforms, ISME J, 2012

Cary, S. C., McDonald, I. R., Barrett, J. E., and Cowan, D. A.: On the rocks: the microbiology of Antarctic Dry Valley soils, Nat Rev Microbiol, 8, 129-138, 10.1038/nrmicro2281, 2010.

Darrah, P. R.: Models of the Rhizosphere .1. Microbial-Population Dynamics around a Root Releasing Soluble and Insoluble Carbon, Plant Soil, 133, 187-199, Doi 10.1007/Bf00009191, 1991.

Dessert, C., Dupre, B., Gaillardet, J., Francois, L. M., and Allegre, C. J.: Basalt weathering laws and the impact of basalt weathering on the global carbon cycle, Chem Geol, 202, 257-273, DOI 10.1016/j.chemgeo.2002.10.001, 2003.

Duc, L., Noll, M., Meier, B. E., Burgmann, H., and Zeyer, J.: High Diversity of Diazotrophs in the Forefield of a Receding Alpine Glacier, Microbial Ecol, 57, 179-190, DOI 10.1007/s00248-008-9408-5, 2009.

Dyurgerov, M. B., and Meier, M. F.: Twentieth century climate change: Evidence from small glaciers, P Natl Acad Sci USA, 97, 1406-1411, DOI 10.1073/pnas.97.4.1406, 2000.

Edgar, R. C., Haas, B. J., Clemente, J. C., Quince, C., and Knight, R.: UCHIME improves sensitivity and speed of chimera detection, Bioinformatics, 27, 2194-2200, 10.1093/bioinformatics/btr381, 2011.

848   Ensign, K. L., Webb, E. A., and Longstaffe, F. J.: Microenvironmental and seasonal variations
849   in soil water content of the unsaturated zone of a sand dune system at Pinery Provincial Park,
850   Ontario, Canada, Geoderma, 136, 788-802, DOI 10.1016/j.geoderma.2006.06.009, 2006.
851   Esperschutz, J., Perez-de-Mora, A., Schreiner, K., Welzl, G., Buegger, F., Zeyer, J., Hagedorn,
852   F., Munch, J. C., and Schloter, M.: Microbial food web dynamics along a soil chronosequence
853   of a glacier forefield, Biogeosciences, 8, 3283-3294, DOI 10.5194/bg-8-3283-2011, 2011.
854   Fleming, K. M., Dowdeswell, J. A., and Oerlemans, J.: Modelling the mass balance of northwest
855   Spitsbergen glaciers and responses to climate change, Annals of Glaciology, Vol 24, 1997, 24,
856   203-210, 1997.
857   Foereid, B., and Yearsley, J. M.: Modelling the impact of microbial grazers on soluble
858   rhizodeposit turnover, Plant Soil, 267, 329-342, DOI 10.1007/s11104-005-0139-9, 2004.
859   Frey, B., Rieder, S. R., Brunner, I., Plotze, M., Koetzsch, S., Lapanje, A., Brandl, H., and Furrer,
860   G.: Weathering-Associated Bacteria from the Damma Glacier Forefield: Physiological
861   Capabilities and Impact on Granite Dissolution, Appl Environ Microb, 76, 4788-4796, Doi
862   10.1128/Aem.00657-10, 2010.
863   Frey, B., Buhler, L., Schmutz, S., Zumsteg, A., and Furrer, G.: Molecular characterization of
864   phototrophic microorganisms in the forefield of a receding glacier in the Swiss Alps, Environ
865   Res Lett, 8, Artn 015033
866   Doi 10.1088/1748-9326/8/1/015033, 2013.
867   Galloway, J. N., Townsend, A. R., Erisman, J. W., Bekunda, M., Cai, Z. C., Freney, J. R.,
868   Martinelli, L. A., Seitzinger, S. P., and Sutton, M. A.: Transformation of the nitrogen cycle:
869   Recent trends, questions, and potential solutions, Science, 320, 889-892,
870   10.1126/science.1136674, 2008.
871   Geng, L., Alexander, B., Cole-Dai, J., Steig, E. J., Savarino, J., Sofen, E. D., and Schauer, A. J.:
872   Nitrogen isotopes in ice core nitrate linked to anthropogenic atmospheric acidity change, P
873   Natl Acad Sci USA, 111, 5808-5812, 10.1073/pnas.1319441111, 2014.
874   Goransson, H., Venterink, H. O., and Baath, E.: Soil bacterial growth and nutrient limitation
875   along a chronosequence from a glacier forefield, Soil Biol Biochem, 43, 1333-1340, DOI
876   10.1016/j.soilbio.2011.03.006, 2011.
877   Guelland, K., Esperschutz, J., Bornhauser, D., Bernasconi, S. M., Kretzschmar, R., and
878   Hagedorn, F.: Mineralisation and leaching of C from C-13 labelled plant litter along an initial
879   soil chronosequence of a glacier forefield, Soil Biol Biochem, 57, 237-247, DOI
880   10.1016/j.soilbio.2012.07.002, 2013a.
881   Guelland, K., Hagedorn, F., Smittenberg, R. H., Goransson, H., Bernasconi, S. M., Hajdas, I.,
882   and Kretzschmar, R.: Evolution of carbon fluxes during initial soil formation along the forefield
883   of Damma glacier, Switzerland, Biogeochemistry, 113, 545-561, DOI 10.1007/s10533-012-
884   9785-1, 2013b.
885   Hamilton, T. L., Peters, J. W., Skidmore, M. L., and Boyd, E. S.: Molecular evidence for an active
886   endogenous microbiome beneath glacial ice, Isme J, 7, 1402-1412, 10.1038/ismej.2013.31,
887   2013.
888   Hellweger, F. L., and Bucci, V.: A bunch of tiny individuals-Individual-based modeling for
889   microbes, Ecol Model, 220, 8-22, DOI 10.1016/j.ecolmodel.2008.09.004, 2009.
890   Hodkinson, I. D., Coulson, S. J., and Webb, N. R.: Community assembly along proglacial
891   chronosequences in the high Arctic: vegetation and soil development in north-west Svalbard,
892   J Ecol, 91, 651-663, DOI 10.1046/j.1365-2745.2003.00786.x, 2003.
893   Hodson, A., Anesio, A. M., Ng, F., Watson, R., Quirk, J., Irvine-Fynn, T., Dye, A., Clark, C.,
894   McCloy, P., Kohler, J., and Sattler, B.: A glacier respires: Quantifying the distribution and

respiration CO2 flux of cryoconite across an entire Arctic supraglacial ecosystem, J Geophys Res-Biogeo, 112, Artn G04s36
Doi 10.1029/2007jg000452, 2007.

Hodson, A., Roberts, T. J., Engvall, A. C., Holmen, K., and Mumford, P.: Glacier ecosystem response to episodic nitrogen enrichment in Svalbard, European High Arctic, Biogeochemistry, 98, 171-184, DOI 10.1007/s10533-009-9384-y, 2010.

Hodson, A. J., Mumford, P. N., Kohler, J., and Wynn, P. M.: The High Arctic glacial ecosystem: new insights from nutrient budgets, Biogeochemistry, 72, 233-256, DOI 10.1007/s10533-004-0362-0, 2005.

Ingwersen, J., Poll, C., Streck, T., and Kandeler, E.: Micro-scale modelling of carbon turnover driven by microbial succession at a biogeochemical interface, Soil Biol Biochem, 40, 864-878, DOI 10.1016/j.soilbio.2007.10.018, 2008.

Insam, H., and Haselwandter, K.: Metabolic Quotient of the Soil Microflora in Relation to Plant Succession, Oecologia, 79, 174-178, Doi 10.1007/Bf00388474, 1989.

Jakubas, D., Zmudczynska, K., Wojczulanis-Jakubas, K., and Stempniewicz, L.: Faeces deposition and numbers of vertebrate herbivores in the vicinity of planktivorous and piscivorous seabird colonies in Hornsund, Spitsbergen, Pol Polar Res, 29, 45-58, 2008.

Jessup, C. M., Kassen, R., Forde, S. E., Kerr, B., Buckling, A., Rainey, P. B., and Bohannan, B. J. M.: Big questions, small worlds: microbial model systems in ecology, Trends Ecol Evol, 19, 189-197, 10.1016/j.tree.2004.01.008, 2004.

Johannessen, O. M., Bengtsson, L., Miles, M. W., Kuzmina, S. I., Semenov, V. A., Alekseev, G. V., Nagurnyi, A. P., Zakharov, V. F., Bobylev, L. P., Pettersson, L. H., Hasselmann, K., and Cattle, A. P.: Arctic climate change: observed and modelled temperature and sea-ice variability, Tellus A, 56, 328-341, DOI 10.1111/j.1600-0870.2004.00060.x, 2004.

Kastovska, K., Elster, J., Stibal, M., and Santruckova, H.: Microbial assemblages in soil microbial succession after glacial retreat in Svalbard (high Arctic), Microbial Ecol, 50, 396-407, DOI 10.1007/s00248-005-0246-4, 2005.

King, A. J., Meyer, A. F., and Schmidt, S. K.: High levels of microbial biomass and activity in unvegetated tropical and temperate alpine soils, Soil Biol Biochem, 40, 2605-2610, DOI 10.1016/j.soilbio.2008.06.026, 2008.

Kirchman, D.: Measuring Bacterial Biomass Production and Growth Rates from Leucine Incorporation in Natural Aquatic Environments in: Marine Microbiology, edited by: Paul, J. H., Academic Press, London, UK, 2001.

Knapp, E. B., Elliott, L. F., and Campbell, G. S.: Carbon, Nitrogen and Microbial Biomass Interrelationships during the Decomposition of Wheat Straw - a Mechanistic Simulation-Model, Soil Biol Biochem, 15, 455-461, Doi 10.1016/0038-0717(83)90011-1, 1983.

Kuhnel, R., Roberts, T. J., Bjorkman, M. P., Isaksson, E., Aas, W., Holmen, K., and Strom, J.: 20-Year Climatology of NO3- and NH4+ Wet Deposition at Ny-Alesund, Svalbard, Adv Meteorol, Artn 406508
Doi 10.1155/2011/406508, 2011.

Kuhnel, R., Bjorkman, M. P., Vega, C. P., Hodson, A., Isaksson, E., and Strom, J.: Reactive nitrogen and sulphate wet deposition at Zeppelin Station, Ny-Alesund, Svalbard, Polar Res, 32, Unsp 19136
Doi 10.3402/Polar.V32i0.19136, 2013.

Larsen, P., Hamada, Y., and Gilbert, J.: Modeling microbial communities: Current, developing, and future technologies for predicting microbial community interaction, J Biotechnol, 160, 17-24, 10.1016/j.jbiotec.2012.03.009, 2012.

942 Lazzaro, A., Brankatschk, R., and Zeyer, J.: Seasonal dynamics of nutrients and bacterial
943 communities in unvegetated alpine glacier forefields, Appl Soil Ecol, 53, 10-22, DOI
944 10.1016/j.apsoil.2011.10.013, 2012.

945 Lazzaro, A., Hilfiker, D., and Zeyer, J.: Structures of Microbial Communities in Alpine Soils:
946 Seasonal and Elevational Effects, Frontiers in microbiology, 6, ARTN 1330
947 10.3389/fmicb.2015.01330, 2015.

948 Lee, S.: A theory for polar amplification from a general circulation perspective, Asia-Pac J
949 Atmos Sci, 50, 31-43, DOI 10.1007/s13143-014-0024-7, 2014.

950 Luoto, T. P., Oksman, M., and Ojala, A. E. K.: Climate change and bird impact as drivers of High
951 Arctic pond deterioration, Polar Biol, 38, 357-368, 10.1007/s00300-014-1592-9, 2015.

952 Lutz, S., Anesio, A. M., Villar, S. E. J., and Benning, L. G.: Variations of algal communities cause
953 darkening of a Greenland glacier, Fems Microbiol Ecol, 89, 402-414, 10.1111/1574-
954 6941.12351, 2014.

955 Lutz, S., Anesio, A. M., Edwards, A., and Benning, L. G.: Microbial diversity on Icelandic glaciers
956 and ice caps, Frontiers in microbiology, 6, ARTN 307
957 10.3389/fmicb.2015.00307, 2015.

958 Manzoni, S., Porporato, A., D'Odorico, P., Laio, F., and Rodriguez-Iturbe, I.: Soil nutrient cycles
959 as a nonlinear dynamical system, Nonlinear Proc Geoph, 11, 589-598, 2004.

960 Manzoni, S., and Porporato, A.: A theoretical analysis of nonlinearities and feedbacks in soil
961 carbon and nitrogen cycles, Soil Biol Biochem, 39, 1542-1556, 10.1016/j.soilbio.2007.01.006,
962 2007.

963 Mapelli, F., Marasco, R., Rizzi, A., Baldi, F., Ventura, S., Daffonchio, D., and Borin, S.: Bacterial
964 Communities Involved in Soil Formation and Plant Establishment Triggered by Pyrite
965 Bioweathering on Arctic Moraines, Microbial Ecol, 61, 438-447, 10.1007/s00248-010-9758-7,
966 2011.

967 McDonald, D., Price, M. N., Goodrich, J., Nawrocki, E. P., DeSantis, T. Z., Probst, A., Andersen,
968 G. L., Knight, R., and Hugenholtz, P.: An improved Greengenes taxonomy with explicit ranks
969 for ecological and evolutionary analyses of bacteria and archaea, Isme J, 6, 610-618,
970 10.1038/ismej.2011.139, 2012.

971 Michelutti, N., Keatley, B. E., Brimble, S., Blais, J. M., Liu, H. J., Douglas, M. S. V., Mallory, M.
972 L., Macdonald, R. W., and Smol, J. P.: Seabird-driven shifts in Arctic pond ecosystems, P Roy
973 Soc B-Biol Sci, 276, 591-596, 10.1098/rspb.2008.1103, 2009.

974 Michelutti, N., Mallory, M. L., Blais, J. M., Douglas, M. S. V., and Smol, J. P.: Chironomid
975 assemblages from seabird-affected High Arctic ponds, Polar Biol, 34, 799-812,
976 10.1007/s00300-010-0934-5, 2011.

977 Mindl, B., Anesio, A. M., Meirer, K., Hodson, A. J., Laybourn-Parry, J., Sommaruga, R., and
978 Sattler, B.: Factors influencing bacterial dynamics along a transect from supraglacial runoff to
979 proglacial lakes of a high Arctic glacieri (vol 7, pg 307, 2007), Fems Microbiol Ecol, 59, 762-
980 762, DOI 10.1111/j.1574-6941.2007.00295.x, 2007.

981 Moe, B., Stempniewicz, L., Jakubas, D., Angelier, F., Chastel, O., Dinessen, F., Gabrielsen, G.
982 W., Hanssen, F., Karnovsky, N. J., Ronning, B., Welcker, J., Wojczulanis-Jakubas, K., and Bech,
983 C.: Climate change and phenological responses of two seabird species breeding in the high-
984 Arctic, Mar Ecol Prog Ser, 393, 235-246, 10.3354/meps08222, 2009.

985 Moreau, M., Mercier, D., Laffly, D., and Roussel, E.: Impacts of recent paraglacial dynamics on
986 plant colonization: A case study on Midtre Lovenbreen foreland, Spitsbergen (79 degrees N),
987 Geomorphology, 95, 48-60, DOI 10.1016/j.geomorph.2006.07.031, 2008.

Moritz, R. E., Bitz, C. M., and Steig, E. J.: Dynamics of recent climate change in the Arctic, Science, 297, 1497-1502, DOI 10.1126/science.1076522, 2002.

Paul, F., Frey, H., and Le Bris, R.: A new glacier inventory for the European Alps from Landsat TM scenes of 2003: challenges and results, Ann Glaciol, 52, 144-152, 2011.

Prietzel, J., Dumig, A., Wu, Y. H., Zhou, J., and Klysubun, W.: Synchrotron-based P K-edge XANES spectroscopy reveals rapid changes of phosphorus speciation in the topsoil of two glacier foreland chronosequences, Geochim Cosmochim Ac, 108, 154-171, DOI 10.1016/j.gca.2013.01.029, 2013.

Schipper, L. A., Hobbs, J. K., Rutledge, S., and Arcus, V. L.: Thermodynamic theory explains the temperature optima of soil microbial processes and high Q(10) values at low temperatures, Global Change Biol, 20, 3578-3586, Doi 10.1111/Gcb.12596, 2014.

Schloss, P. D., Westcott, S. L., Ryabin, T., Hall, J. R., Hartmann, M., Hollister, E. B., Lesniewski, R. A., Oakley, B. B., Parks, D. H., Robinson, C. J., Sahl, J. W., Stres, B., Thallinger, G. G., Van Horn, D. J., and Weber, C. F.: Introducing mothur: Open-Source, Platform-Independent, Community-Supported Software for Describing and Comparing Microbial Communities, Appl Environ Microb, 75, 7537-7541, 10.1128/Aem.01541-09, 2009.

Schmidt, S. K., Reed, S. C., Nemergut, D. R., Grandy, A. S., Cleveland, C. C., Weintraub, M. N., Hill, A. W., Costello, E. K., Meyer, A. F., Neff, J. C., and Martin, A. M.: The earliest stages of ecosystem succession in high-elevation (5000 metres above sea level), recently deglaciated soils, P Roy Soc B-Biol Sci, 275, 2793-2802, DOI 10.1098/rspb.2008.0808, 2008.

Schostag, M., Stibal, M., Jacobsen, C. S., Baelum, J., Tas, N., Elberling, B., Jansson, J. K., Semenchuk, P., and Prieme, A.: Distinct summer and winter bacterial communities in the active layer of Svalbard permafrost revealed by DNA- and RNA-based analyses, Frontiers in microbiology, 6, ARTN 399
10.3389/fmicb.2015.00399, 2015.

Schulz, S., Brankatschk, R., Dumig, A., Kogel-Knabner, I., Schloter, M., and Zeyer, J.: The role of microorganisms at different stages of ecosystem development for soil formation, Biogeosciences, 10, 3983-3996, DOI 10.5194/bg-10-3983-2013, 2013.

Schutte, U. M. E., Abdo, Z., Bent, S. J., Williams, C. J., Schneider, G. M., Solheim, B., and Forney, L. J.: Bacterial succession in a glacier foreland of the High Arctic, Isme J, 3, 1258-1268, DOI 10.1038/ismej.2009.71, 2009.

Scott, E. M., Rattray, E. A. S., Prosser, J. I., Killham, K., Glover, L. A., Lynch, J. M., and Bazin, M. J.: A Mathematical-Model for Dispersal of Bacterial Inoculants Colonizing the Wheat Rhizosphere, Soil Biol Biochem, 27, 1307-1318, Doi 10.1016/0038-0717(95)00050-O, 1995.

Serreze, M. C., Walsh, J. E., Chapin, F. S., Osterkamp, T., Dyurgerov, M., Romanovsky, V., Oechel, W. C., Morison, J., Zhang, T., and Barry, R. G.: Observational evidence of recent change in the northern high-latitude environment, Climatic Change, 46, 159-207, Doi 10.1023/A:1005504031923, 2000.

Servedio, M. R., Brandvain, Y., Dhole, S., Fitzpatrick, C. L., Goldberg, E. E., Stern, C. A., Van Cleve, J., and Yeh, D. J.: Not just a theory--the utility of mathematical models in evolutionary biology, Plos Biol, 12, e1002017, 10.1371/journal.pbio.1002017, 2014.

Simon, M., and Azam, F.: Protein-Content and Protein-Synthesis Rates of Planktonic Marine-Bacteria, Mar Ecol Prog Ser, 51, 201-213, DOI 10.3354/meps051201, 1989.

Smittenberg, R. H., Gierga, M., Goransson, H., Christl, I., Farinotti, D., and Bernasconi, S. M.: Climate-sensitive ecosystem carbon dynamics along the soil chronosequence of the Damma glacier forefield, Switzerland, Global Change Biol, 18, 1941-1955, DOI 10.1111/j.1365-2486.2012.02654.x, 2012.

Soetaert, K., and Herman, P.: A Practical Guide to Ecological Modelling: Using R as a Simulation Platform, Springer, UK, 2009.

Staines, K. E. H., Carrivick, J. L., Tweed, F. S., Evans, A. J., Russell, A. J., Jóhannesson, T., and Roberts, M.: A multi-dimensional analysis of pro-glacial landscape change at Sólheimajökull, southern Iceland, Earth Surface Processes and Landforms, 40, 809-822, 10.1002/esp.3662, 2014.

Stapleton, L. M., Crout, N. M. J., Sawstrom, C., Marshall, W. A., Poulton, P. R., Tye, A. M., and Laybourn-Parry, J.: Microbial carbon dynamics in nitrogen amended Arctic tundra soil: Measurement and model testing, Soil Biol Biochem, 37, 2088-2098, DOI 10.1016/j.soilbio.2005.03.016, 2005.

Stibal, M., Tranter, M., Benning, L. G., and Rehak, J.: Microbial primary production on an Arctic glacier is insignificant in comparison with allochthonous organic carbon input, Environ Microbiol, 10, 2172-2178, 10.1111/j.1462-2920.2008.01620.x, 2008.

Strauss, S. L., Garcia-Pichel, F., and Day, T. A.: Soil microbial carbon and nitrogen transformations at a glacial foreland on Anvers Island, Antarctic Peninsula, Polar Biol, 35, 1459-1471, DOI 10.1007/s00300-012-1184-5, 2012.

Telling, J., Anesio, A. M., Tranter, M., Irvine-Fynn, T., Hodson, A., Butler, C., and Wadham, J.: Nitrogen fixation on Arctic glaciers, Svalbard, J Geophys Res-Biogeo, 116, Artn G03039 Doi 10.1029/2010jg001632, 2011.

Telling, J., Stibal, M., Anesio, A. M., Tranter, M., Nias, I., Cook, J., Bellas, C., Lis, G., Wadham, J. L., Sole, A., Nienow, P., and Hodson, A.: Microbial nitrogen cycling on the Greenland Ice Sheet, Biogeosciences, 9, 2431-2442, 10.5194/bg-9-2431-2012, 2012.

Toal, M. E., Yeomans, C., Killham, K., and Meharg, A. A.: A review of rhizosphere carbon flow modelling, Plant Soil, 222, 263-281, Doi 10.1023/A:1004736021965, 2000.

Tscherko, D., Rustemeier, J., Richter, A., Wanek, W., and Kandeler, E.: Functional diversity of the soil microflora in primary succession across two glacier forelands in the Central Alps, Eur J Soil Sci, 54, 685-696, DOI 10.1046/j.1365-2389.2003.00570.x, 2003.

Vandewerf, H., and Verstraete, W.: Estimation of Active Soil Microbial Biomass by Mathematical-Analysis of Respiration Curves - Development and Verification of the Model, Soil Biol Biochem, 19, 253-260, Doi 10.1016/0038-0717(87)90006-X, 1987.

Wang, Y. P., Chen, B. C., Wieder, W. R., Leite, M., Medlyn, B. E., Rasmussen, M., Smith, M. J., Agusto, F. B., Hoffman, F., and Luo, Y. Q.: Oscillatory behavior of two nonlinear microbial models of soil carbon decomposition, Biogeosciences, 11, 1817-1831, 10.5194/bg-11-1817-2014, 2014.

Yde, J. C., Finster, K. W., Raiswell, R., Steffensen, J. P., Heinemeier, J., Olsen, J., Gunnlaugsson, H. P., and Nielsen, O. B.: Basal ice microbiology at the margin of the Greenland ice sheet, Ann Glaciol, 51, 71-79, 2010.

Yoshitake, S., Uchida, M., Koizumi, H., Kanda, H., and Nakatsubo, T.: Production of biological soil crusts in the early stage of primary succession on a High Arctic glacier foreland, New Phytol, 186, 451-460, DOI 10.1111/j.1469-8137.2010.03180.x, 2010.

Zdanowski, M. K., Zmuda-Baranowska, M. J., Borsuk, P., Swiatecki, A., Gorniak, D., Wolicka, D., Jankowska, K. M., and Grzesiak, J.: Culturable bacteria community development in postglacial soils of Ecology Glacier, King George Island, Antarctica, Polar Biol, 36, 511-527, DOI 10.1007/s00300-012-1278-0, 2013.

Zelenev, V. V., van Bruggen, A. H. C., and Semenov, A. M.: "BACWAVE," a spatial-temporal model for traveling waves of bacterial populations in response to a moving carbon source in soil, Microbial Ecol, 40, 260-272, 2000.

1082 Zhang, X. Y., Wang, W., Chen, W. L., Zhang, N. L., and Zeng, H.: Comparison of Seasonal Soil
1083 Microbial Process in Snow-Covered Temperate Ecosystems of Northern China, Plos One, 9,
1084 ARTN e92985
1085 10.1371/journal.pone.0092985, 2014.
1086 Ziolek, M., and Melke, J.: The impact of seabirds on the content of various forms of
1087 phosphorus in organic soils of the Bellsund coast, western Spitsbergen, Polar Res, 33, ARTN
1088 19986
1089 10.3402/polar.v33.19986, 2014.
1090 Zumsteg, A., Bernasconi, S. M., Zeyer, J., and Frey, B.: Microbial community and activity shifts
1091 after soil transplantation in a glacier forefield, Appl Geochem, 26, S326-S329, DOI
1092 10.1016/j.apgeochem.2011.03.078, 2011.
1093 Zumsteg, A., Luster, J., Goransson, H., Smittenberg, R. H., Brunner, I., Bernasconi, S. M., Zeyer,
1094 J., and Frey, B.: Bacterial, Archaeal and Fungal Succession in the Forefield of a Receding
1095 Glacier, Microbial Ecol, 63, 552-564, DOI 10.1007/s00248-011-9991-8, 2012.
1096 Zumsteg, A., Schmutz, S., and Frey, B.: Identification of biomass utilizing bacteria in a carbon-
1097 depleted glacier forefield soil by the use of 13C DNA stable isotope probing, Env Microbiol
1098 Rep, 5, 424-437, Doi 10.1111/1758-2229.12027, 2013.
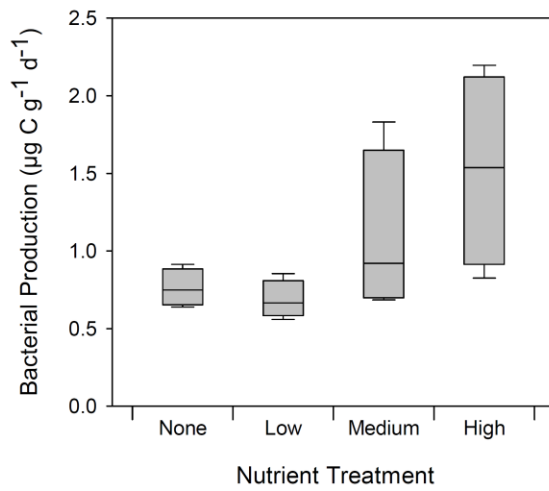1099
1100
1101
1102
1103
1104
1105
1106

1107
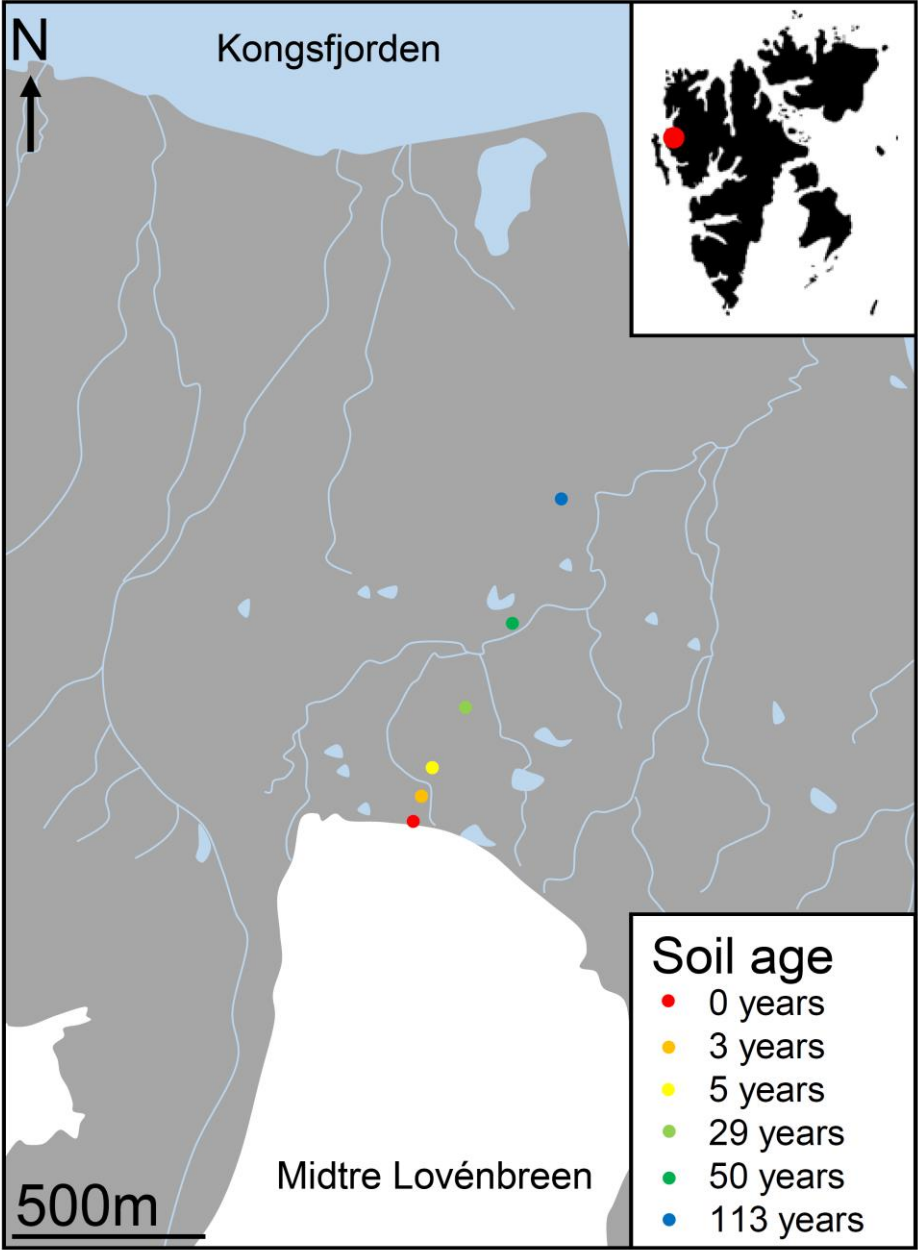
1108

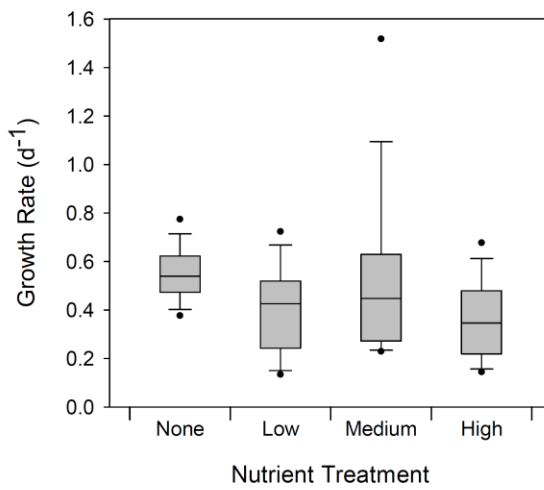1109   Figure 1. Midtre Lovénbreen glacier and forefield in Svalbard, the location of sampling sites and
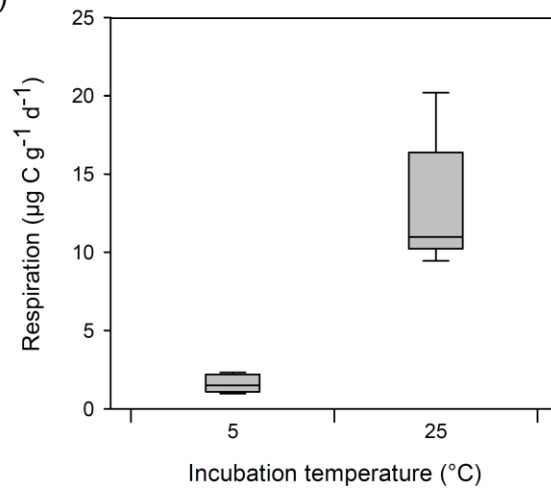
1110   approximate age of soil.

1111

(a)

(b)

(c)
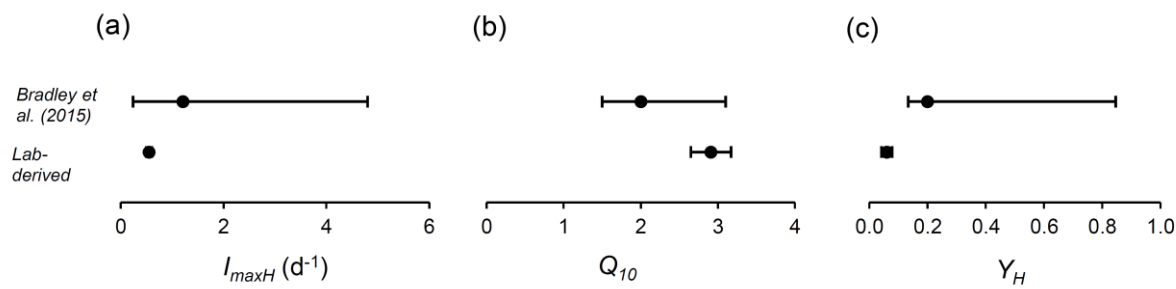

1112

1113 Figure 2. Measurements of (a) bacterial carbon production and (b) growth rate, derived from ^{3}H-leucine

1114 assays at different nutrient conditions, and (c) bacterial respiration at 5°C and 25°C.

1115

1116

1117

1118
1119
1120
1121 Figure 3. A comparison of previously established ranges for parameters (Bradley et al., 2015) with
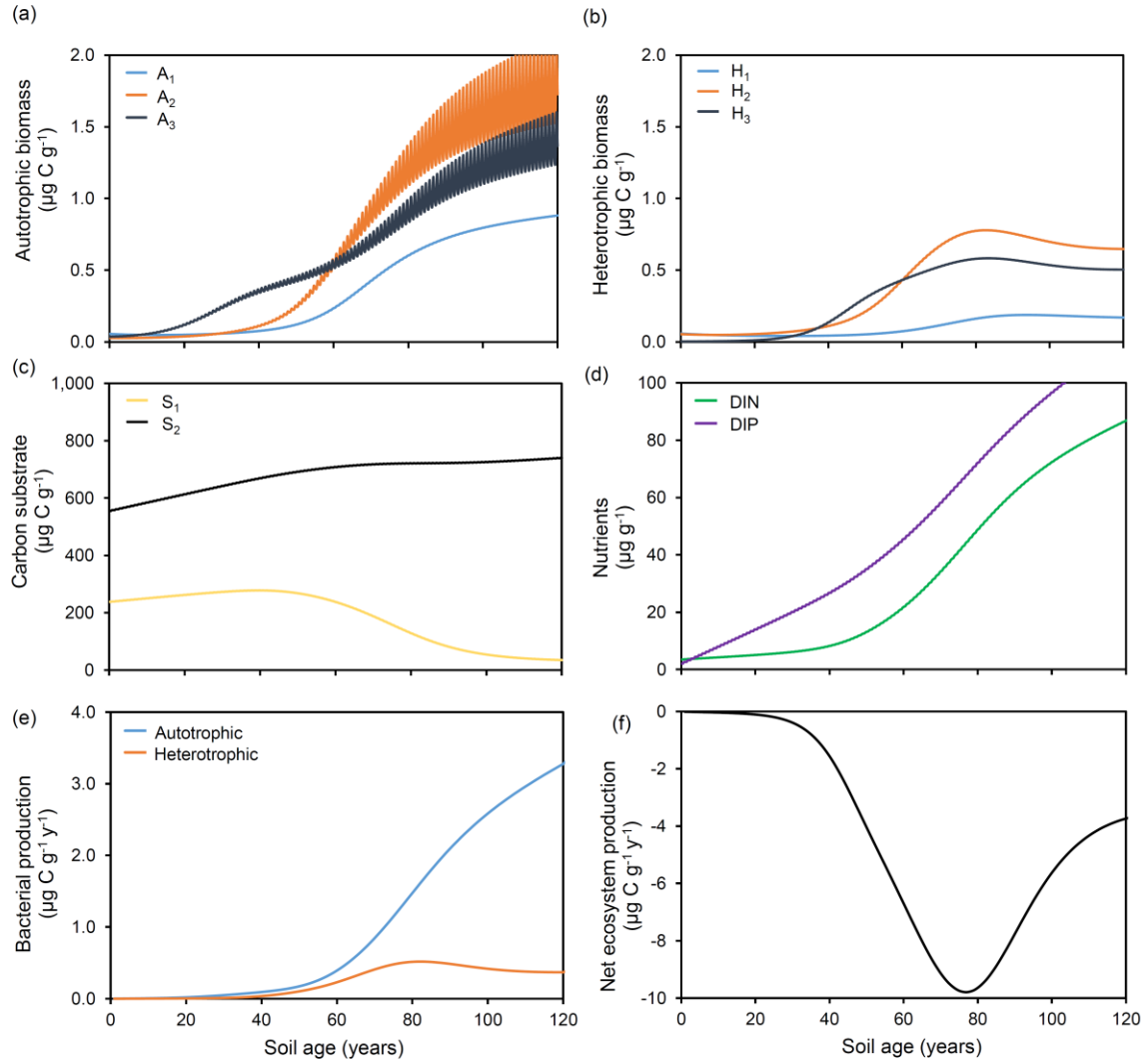1122 laboratory-derived values for (a) maximum growth rate (I_{max}), (b) temperature response (Q_{10}), (c) BGE
1123 (Y).
1124

Figure 4. Modelled (a) autotrophic biomass, (b) heterotrophic biomass, (c) carbon substrate, (d) nutrients, (e) bacterial production and (f) net ecosystem production, with laboratory-derived parameter values.
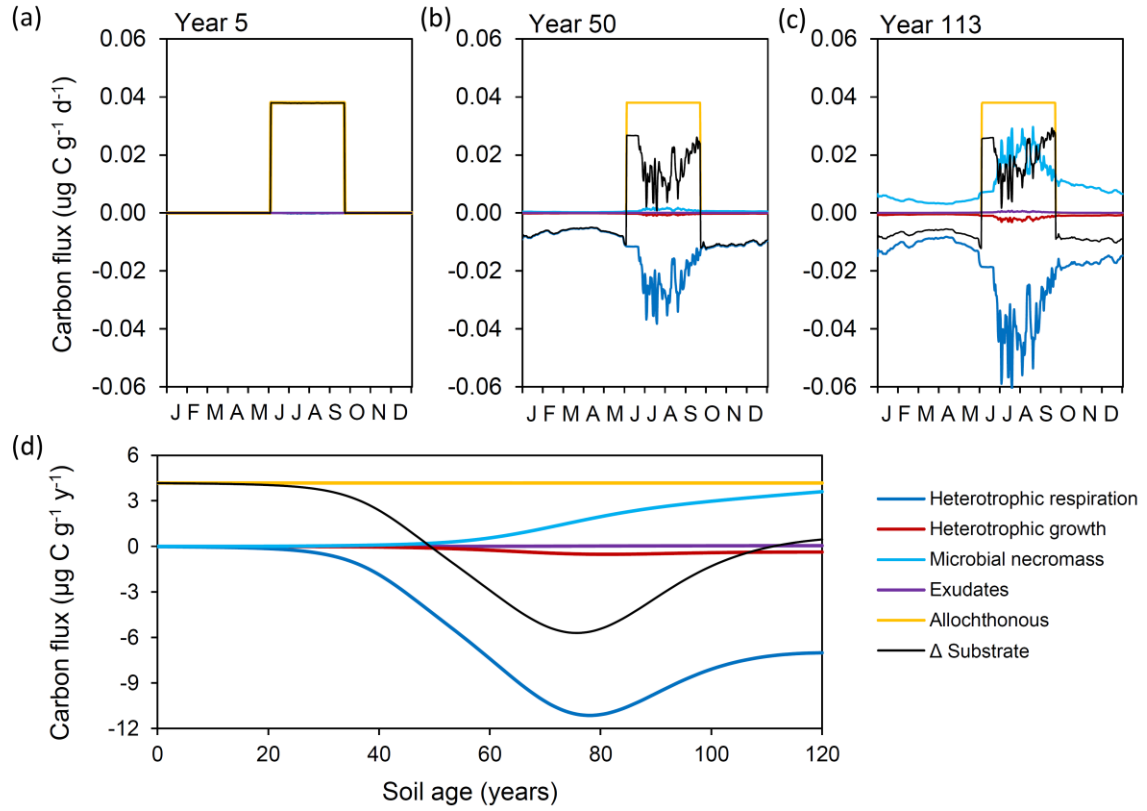
Figure 5. Illustration of daily carbon fluxes for (a) 5, (b) 50 and (c) 113 year old soil, and (d) annual carbon flux over 120 years. Microbial necromass (light blue), exudates (purple) and allochthonous sources (yellow) contribute to the substrate pool (black), and heterotrophic growth (red) and respiration (dark blue) deplete it.
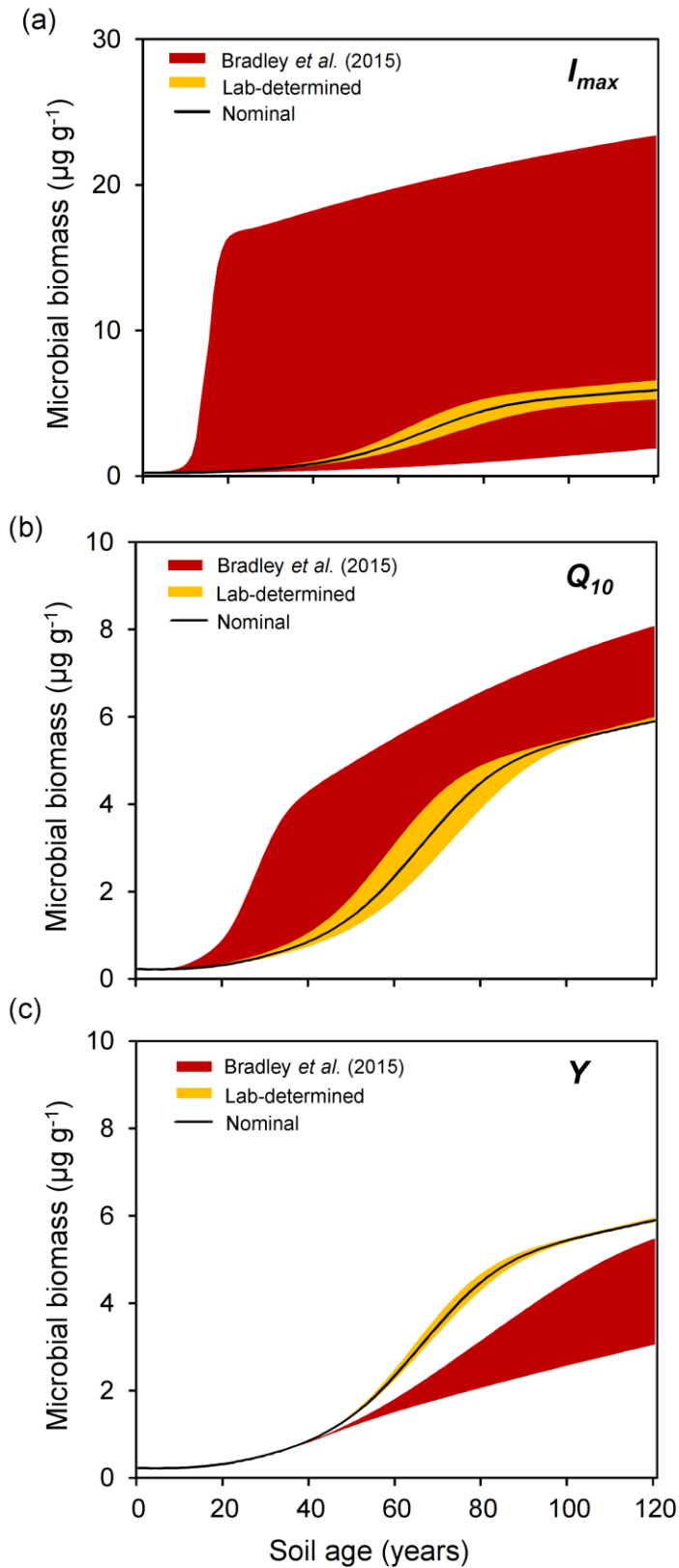
Figure 6. A comparison of predicted microbial biomass with laboratory-derived parameter values (yellow) and previously established parameter values (Bradley et al., 2015) (red) for variation in the following parameters: (a) maximum growth rate (I_{max}), (b) temperature response (Q_{10}), (c) BGE (Y).
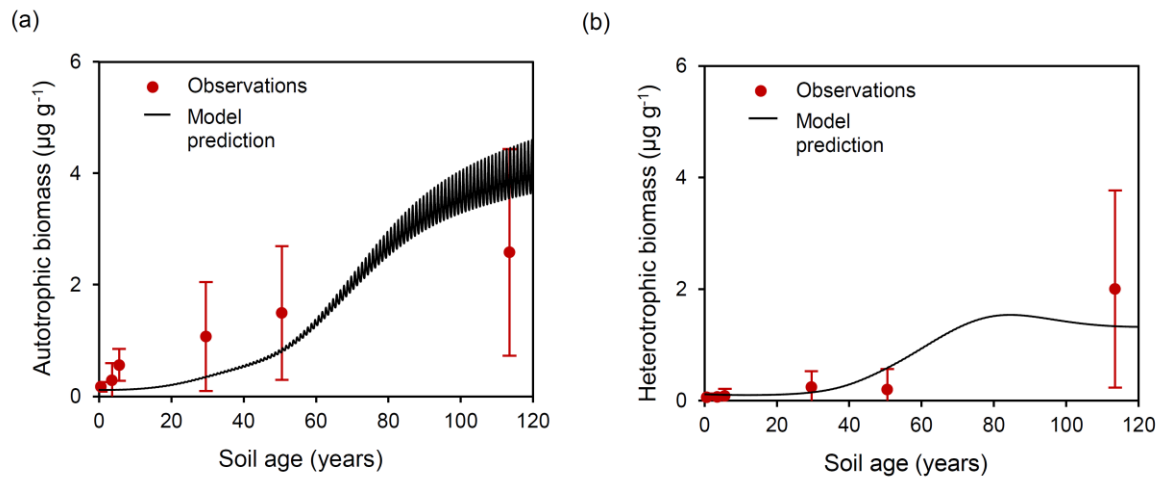
1141

Figure 7. Model predictions of (a) autotrophic and (b) heterotrophic biomass (black line), compared to observational data (red) derived from microscopy.
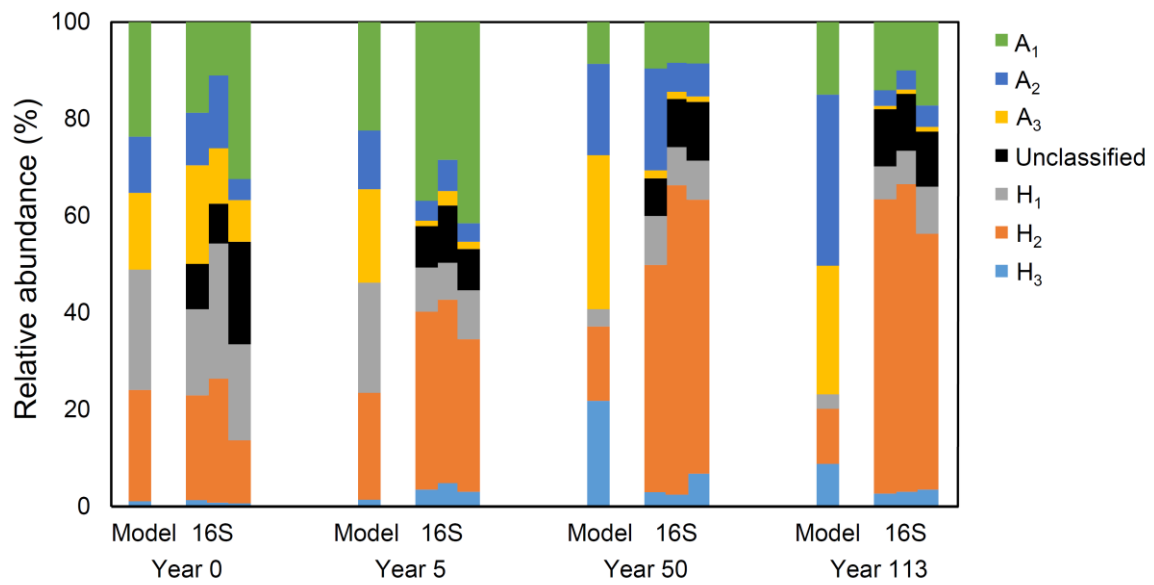
1142
1143
1144

Figure 8. A comparison of microbial diversity from model output and genomic analyses at 0 year old, 5 year old, 50 year old and 113 year old soil.

1151

1152   Table 1. State variables and initial values.

State Variable	Units	Description	Initial value (year 0) ($\mu g\ g^{-1}$)
A_1	$\mu g\ C\ g^{-1}$	Glacial chemolithoautotrophs	0.0547
A_2	$\mu g\ C\ g^{-1}$	Soil autotrophs	0.0266
A_3	$\mu g\ C\ g^{-1}$	Nitrogen fixing soil autotrophs	0.0355
H_1	$\mu g\ C\ g^{-1}$	Glacial heterotrophs	0.0576
H_2	$\mu g\ C\ g^{-1}$	Soil heterotrophs	0.0530
H_3	$\mu g\ C\ g^{-1}$	Nitrogen fixing soil heterotrophs	0.0025
S_1	$\mu g\ C\ g^{-1}$	Labile organic carbon	291.895
S_2	$\mu g\ C\ g^{-1}$	Refractory organic carbon	681.089
DIN	$\mu g\ N\ g^{-1}$	Dissolved inorganic nitrogen (DIN)	3.530
DIP	$\mu g\ P\ g^{-1}$	Dissolved inorganic phosphorus (DIP)	2.078
ON_1	$\mu g\ N\ g^{-1}$	Labile organic nitrogen	41.157
ON_2	$\mu g\ N\ g^{-1}$	Refractory organic nitrogen	96.034
OP_1	$\mu g\ P\ g^{-1}$	Labile organic phosphorus	24.227
OP_2	$\mu g\ P\ g^{-1}$	Refractory organic phosphorus	56.530

1153
1154
1155
1156

1157   Table 2. Microbial biomass in the forefield of Midtre Lovénbreen (brackets show 1 standard deviation)
1158

Soil Age (years)	Autotrophic biomass (µg C g^{-1})		Heterotrophic biomass (µg C g^{-1})		Total Organic Carbon (µg C g^{-1})	
0	0.171	(0.042)	0.059	(0.034)	792.984	(127.206)
3	0.287	(0.155)	0.064	(0.029)		
5	0.561	(0.143)	0.083	(0.065)		
29	1.072	(0.487)	0.244	(0.142)		
50	1.497	(0.601)	0.197	(0.184)		
113	2.581	(0.927)	2.000	(0.885)		

1159
1160
1161
1162
1163
1164

1165   Table 3. Model output.

Soil Age (years)	Autotrophic biomass (µg C g^{-1})	Heterotrophic biomass (µg C g^{-1})	Autotrophic production (µg C g^{-1} y^{-1})	Heterotrophic production (µg C g^{-1} y^{-1})	Net ecosystem production (µg C g^{-1} y^{-1})	DIN assimilation (µg N g^{-1} y^{-1})	N$_2$ fixation (µg N g^{-1} y^{-1})
0	0.117	0.111	0.002	0.001	- 0.011	2.0×10^{-4}	2.0×10^{-4}
3	0.117	0.105	0.003	0.001	- 0.020	3.0×10^{-4}	3.0×10^{-4}
5	0.119	0.102	0.004	0.001	- 0.025	4.0×10^{-4}	4.0×10^{-4}
29	0.359	0.147	0.050	0.012	- 0.391	0.002	0.006
50	0.860	0.591	0.187	0.113	- 4.311	0.022	0.021
113	4.414	1.331	3.093	0.376	- 4.031	0.458	0.031

1166
1167
1168
1169
1170
1171
1172